An *ex vivo* biomechanical study of equine neonatal rib fracture repair by different fixation methods

by

Kayla Newell

A thesis submitted to the Graduate Faculty of
Auburn University
in partial fulfillment of the
requirements for the Degree of
Master's of Science

Auburn, Alabama
August 8, 2026

Keywords: equine, rib fracture, modified reconstruction plate, string of pearls plate, nylon cable tie, rib clip

Approved by

Lindsey Boone, Chair, Joezy Griffin Endowed Professor of Equine Surgery and Sports Medicine
Fred Caldwell, Professor of Equine Surgery and Sports Medicine
Jenna Bayne, Associate Clinical Professor of Farm Animal Medicine and Surgery
Robert Cole, Professor of Radiology

Abstract

Introduction: Rib fractures result in significant morbidity and mortality of equine neonates. Various methods to repair these fractures have been described but biomechanical testing in immature equine neonatal bone has not been performed. The study objective was to compare strength, stiffness, and mode of failure for four different methods of equine neonatal rib fracture repair.

Methods: Equine neonatal cadavers (< 2 weeks of age) without history of dystocia or thoracic trauma present were used for this study. Ribs three through six on both left and right side were randomly allocated to one of four repair groups: nylon cable tie (NCT), modified reconstruction plate (MRP), string of pearls plate (SOP), or rib clip (RC). Intact ribs were first fractured under three-point bending to induce a simple, transverse fracture. The fracture was then reduced and repaired according to the assigned repair group. Repaired ribs were then tested to failure under single-cycle, four-point bending. Strength (maximum force, F_{max}, and force at failure, F_{fail}) and mode of failure were recorded. Stiffness (N/mm^2) was calculated. Data were analyzed using linear mixed models

Results: In intact ribs, no significant differences in F_{max} (P=0.46), F_{fail} (P=0.35), or stiffness (P=0.90) were observed between groups. Among repair groups, F_{max}, F_{fail}, and stiffness differed significantly (P<0.0001). NCT repairs had significantly lower F_{max} and F_{fail} than MRP and SOP, while MRP and SOP had greater stiffness compared to NCT and RC. NCT and RC groups failed at the original fracture site, whereas MRP and SOP failed mostly due to screw pullout.

Conclusion: Rigid fixation with MRP or SOP provides stronger fracture repair than NCT or RC when equine neonatal ribs are tested under single-cycle load to failure. Further investigation of both rigid and non-rigid repair methods with cyclic loading is warranted.

Artificial Intelligence (AI) Use Disclosure Statement

In the preparation of this thesis / dissertation, the following Artificial Intelligence (AI) tools were used: Gemini. This tool was used primarily for grammar and brainstorming. The author acknowledges full responsibility for the intellectual content of this work and has ensured that all AI-assisted sections have been reviewed and revised for accuracy and appropriate academic style. All AI-generated content was reviewed and validated for relevance, appropriateness, and accuracy before incorporation into the final document to maintain scholarly integrity of this research.

Digital Accessibility Disclosure Statement

In the preparation of this thesis / dissertation, no digital accessibility tools were used to ensure this document complies with federal requirements. The author acknowledges full responsibility for the intellectual content of this work and has made a good faith effort to comply with digital accessibility requirements in publishing, wherein the nature of the content does not significantly change in order to do so. Furthermore, all content has been reviewed and revised to meet these requirements prior to final publication.

Acknowledgements

I am profoundly grateful to the many individuals who have shaped my career and guided me to this point. I feel exceptionally fortunate to have been mentored in surgery by extraordinary clinicians, including Drs. Fred Caldwell, Lindsey Boone, Reid Hanson, Claudia Reyner, and Scott McClure. I would like to express my deepest appreciation to my mentor and research advisor, Dr. Lindsey Boone, for introducing me to this master's topic and for providing unwavering guidance and support throughout my graduate studies and residency; this research would not have been possible without her insight. Furthermore, I extend my sincere thanks to Drs. Jenna Bayne, Fred Caldwell, Robert Cole, and Ramis Farag for lending their expertise and direction to this research project. Special thanks go to my co-residents, Drs. Avery Loyd, Mana Okudaira, and Agathe Guillemet, whose camaraderie and assistance were indispensable throughout our training. Finally, I wish to express my heartfelt gratitude to my family and friends for their enduring moral support and motivation during my journey to becoming an equine surgeon.

Table of Contents

List of Tables

List of Figures

List of Abbreviations

NCT= Nylon cable tie

MRP= Modified reconstruction plate

SOP= String of pearls plate

RC= Rip clip

SSRF: Surgical stabilization of rib fracture

Fmax= Maximum force (N) sustained by specimen

Ffail= Force (N) at specimen failure

Chapter 1 Introduction and Literature Review

a. Bone Biology and Fracture Healing

i. Cortical and Cancellous Bone

There are two types of bone, cortical and cancellous bone, that together form every bone in the body. The percent of each bone type changes according to the structure and mechanical needs of the bone. For instance, the bone has three main boney shapes that include long, flat, and cuboidal bones. Long bones are composed mostly of cortical bone and make up the bulk of the appendicular skeleton, being responsible for bearing weight (standing) and body motion. Flat bones are composed mostly of cancellous bone, predominantly found in the axial skeleton, responsible for support and protection of the central nervous system (spinal cord) as well as vital structures of the thorax and abdomen. Cuboidal bones mostly consist of cancellous bone as well, with a thin cortical layer surrounding it. They are considered short bones which receive multidirectional forces and transmit mechanical leverage across complex joints.

The macrostructure of the bone will now be discussed using a long bone compared to a flat bone. A long bone is composed of four different regions: a diaphysis or the middle of the long bone, and moving in order the metaphysis, physis, and epiphysis.[1] Whereas a flat bone, or specifically a rib, consists of a body or shaft, a neck that connects the body to the head, and a tubercle that helps connect the transverse process to the vertebrae.

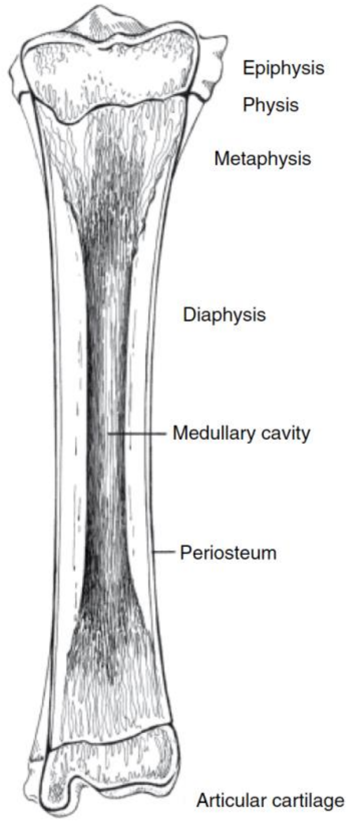

Figure 1Macrostructure of the equine tibia. (Markel, 2019)

The physis of an immature long bone is responsible for mostly longitudinal bone growth through the process of endochondral ossification which ceases when the animal reaches skeletal maturity at approximately 4-5 years for the equid. The metaphysis is the wider, expanded end of each long bone, composed of more cancellous bone than the diaphysis surrounded by cortical bone. Intramembranous ossification occurs in the development of flat bones, such as the rib. Intramembranous ossification is the process where bone forms directly within sheets of mesenchymal connective tissue to create flat bones like the skull and clavicles. The process begins when mesenchymal cells cluster together within the connective tissue membrane and differentiate into osteoblasts to establish an ossification center. These osteoblasts secrete an unmineralized organic matrix called osteoid, which quickly hardens and calcifies as calcium and other mineral salts deposit into it. As the matrix solidifies, trapped osteoblasts differentiate into mature osteocytes, while the surrounding matrix develops into a latticework of bony beams called trabeculae. Blood vessels grow into the spaces between these trabeculae, bringing nutrients and giving rise to red bone marrow. Finally, the remaining mesenchyme on the outside of the bone condenses to form the protective periosteum, beneath which a layer of dense compact bone replaces the superficial spongy layers while leaving the internal spongy core intact.

The bone’s microstructure is composed of three principal components: cells, organic matrix, and inorganic matrix. The cellular components of bone are critical for bone remodeling and adaptation to stress. It consists of osteoblasts, osteocytes, and osteoclasts. Osteoblasts are responsible for formation of the organic matrix, osteoid, which is deposited on bone surfaces. A small percentage of osteoblasts become osteocytes when they become engulfed by osteoid. Osteocytes use cytoplasmic processes to regulate the exchange of mineral ions between extracellular fluid and bone through the canicular system. Howship’s lacunae are bone resorption sites in which osteoclasts reside.

The osteon or Haversian system is a principal unit of a long bone which contains blood vessels, nerve fibers, and lymphatics within lamella of mineralized bone (Figure 2). This central canal provides nutrients to the osteocyte. Collagen fibers within the bone matrix connect the lamella to one another within an osteon increasing bones resistance to stress. Lamellar bone consists of primary osteons formed during appositional growth and is always surrounded by woven bone, and secondary osteons are formed during bone remodeling initiated by osteoclasts. Woven bone is the first type of bone that appears during embryonic development and in a callus during indirect fracture repair. Most woven bone is then replaced by lamellar bone, rearranging the lamellar bundles into parallel or concentric sheets known as indirect bone remodeling.[1] The microstructure of a flat bone resembles a sandwich arrangement, where an internal core of spongy bone, known as the diploë, is securely enclosed between two protective outer layers of dense compact bone. The external and internal surfaces of the compact bone are lined with fibrous membranes called the periosteum and endosteum, respectively, which house osteogenic stem cells, osteoblasts, and osteoclasts essential for bone growth and repair. Unlike long bones, flat bones lack a central medullary cavity and distinct osteon systems; instead, their outer compact layers are composed of parallel lamellae, which are highly organized sheets of mineralized collagen matrix. Trapped within tiny fluid-filled spaces called lacunae between these lamellae are mature osteocytes, which communicate with one another and nearby blood vessels through a network of microscopic canals called canaliculi. Deep within the bone, the spongy diploë is structured as a chaotic, porous latticework of bony struts called trabeculae, which are lined with endosteum and filled with highly vascularized red bone marrow responsible for hematopoiesis, or blood cell production.[59]

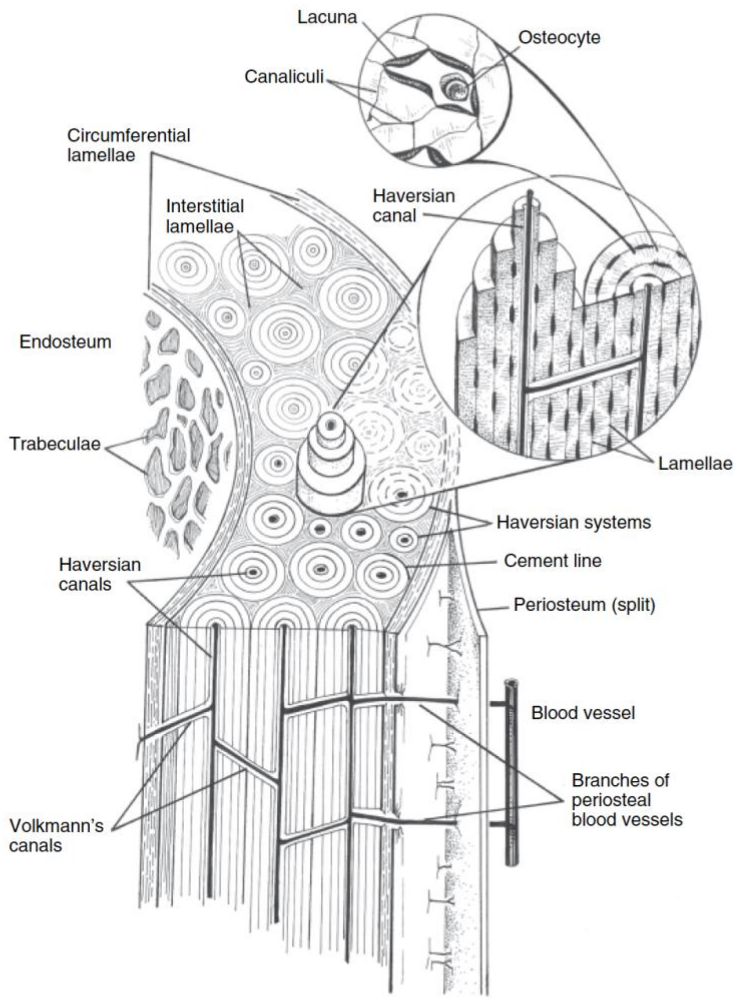

Figure 2 Microstructure of the long bone. (Markel, 2019)

ii. Endochondral and intramembranous ossification

Endochondral ossification occurs during longitudinal bone growth where cartilage is gradually turned into bone. This process is driven by chondrocytes through various organized zones occurring at the physis or the growth plate until skeletal maturity occurs and the physis closes. The zones start at the epiphyseal end of the growth plate and move toward the metaphysis (Figure 3). The process begins in the resting zone, which consists of low-metabolic chondrocytes. In the adjacent proliferation zone, rapid mitosis occurs perpendicular to the bone plane to lengthen the cellular columns. The cells then enter the hypertrophic zone, where they mature and expand within the surrounding extracellular matrix. Finally, in the calcification zone, these hypertrophic chondrocytes remodel and mineralize the matrix, eventually being replaced by osteocytes. Once the physis closes with maturity, the proliferation ceases.[2,3]

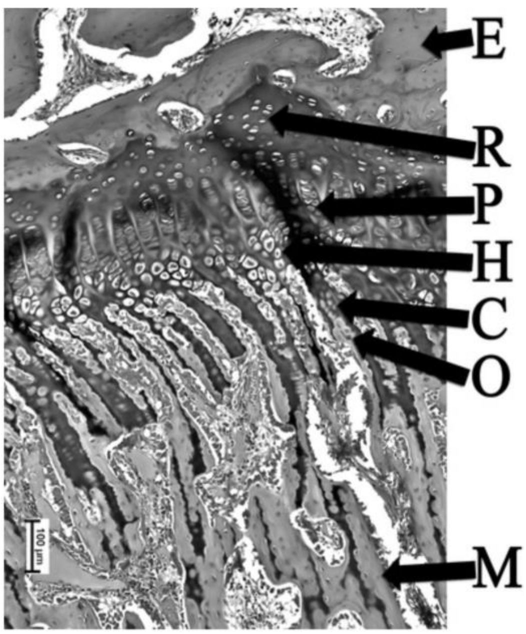

Figure 3 Zones of Endochondral Ossification (E-epiphysis, R-resting zone, P-proliferative zone, H-hypertrophic zone, C-calcification zone, O-ossification zone, M-metaphysis). (Auer, 2018)

Intramembranous ossification forms most of the flat bones within the axial skeleton directly converting skeletal stem and progenitor cells or mesenchymal tissue to bone. Mesenchymal cells first differentiate into osteoblasts, grouping together to form an ossification center. The osteoblasts secrete osteoid which is a collagen proteoglycan matrix. When the osteoid binds with calcium, the matrix hardens, and the osteoblasts become trapped, then turn into osteocytes. The continuation of secretion of osteoid by osteoblasts forms the trabecular bone, and mesenchymal cells on the surface of the bone form the periosteum. Layers of osteoid and osteoblasts are located on the inner surface of the periosteum superficial to and surrounding the more centrally located trabecular bone.[4]

iii. Indirect and direct bone healing mechanisms

Fractures must heal by new bone formation. New bone formation occurs through intramembranous and/or endochondral ossification. Indirect healing occurs when the fracture is not stable due to malalignment and/or motion of the fracture fragments. Indirect bone healing occurs in three stages (Figure 4). First, the inflammatory stage occurs after fracture when a hematoma forms providing a provisional matrix for bone repair. Immune cells, such as neutrophils and macrophages migrate to the fracture site to clean up the tissue damage and release cellular signals such as cytokines, chemokines, and growth factors that will stimulate migration and infiltration of cells responsible for tissue repair. This stage of bone healing is known as the repair stage. Repair cells, such as mesenchymal stem and progenitor cells differentiate into terminally effector cells such as osteoblasts and fibroblasts, invading the provisional matrix of the hematoma forming granulation tissue within 3-5 days. This granulation tissue is transformed into a soft, cartilaginous callus that bridges the fracture fragments. The soft callus then hardens over time through intramembranous ossification, forming a hard callus providing support and strength to the healing fracture site. The last phase of healing is bone remodeling, which starts approximately 3-4 weeks after the fracture and can take several months or even years to complete. The remodeling phase consists of hard callus resorption by osteoclasts and lamellar bone formation by osteoblasts.

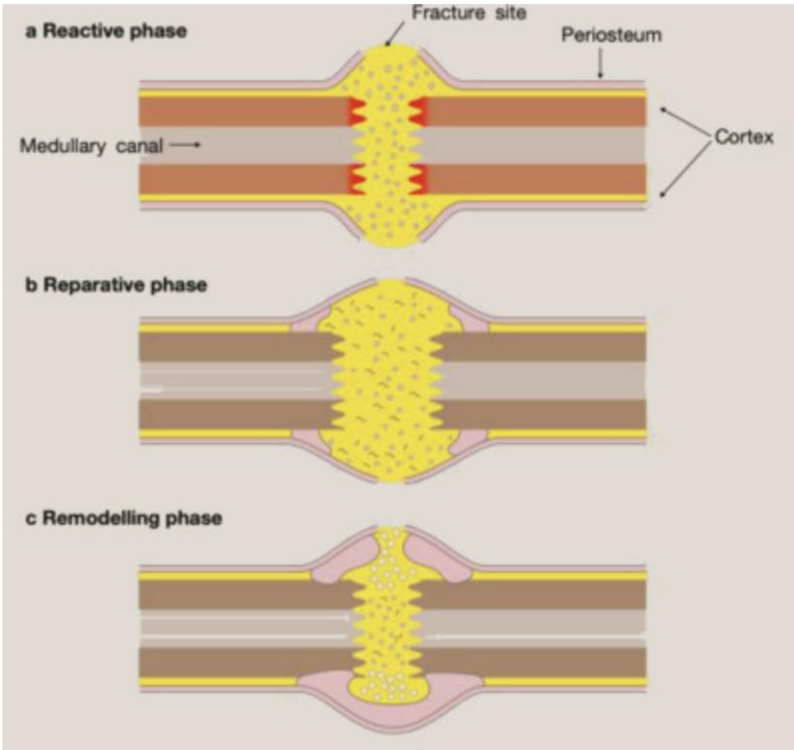

Figure 4 Phases of indirect fracture healing. (Khondi, 2023)

The goal of surgical management when utilizing internal fixation is direct bone healing with limited interfragmentary movement. Direct bone healing using contact healing occurs when the fracture gap is smaller than 0.01mm with less than 2% interfragmentary strain.[5] Close to the fracture site cutting cones contain osteoclasts that generate longitudinal cavities filled with bone by osteoblasts. The bridging osteons are then remodeled into lamellar bone without periosteal callus. Direct bone healing using gap healing occurs when the fracture gap is 800 um to 1mm and lamellar bone perpendicular to the long axis initially fills in the fracture gap. It is then remodeled by cutting cones like contact healing.[2]

b. Equine Fracture Biomechanics

i. Load-deformation Curve

Evaluating bone fracture repair strategies requires a thorough understanding of skeletal biomechanics. Bone breaks according to several factors including material and structural properties of the bone as well as how the load is applied (direction, rate, magnitude, frequency, and duration). In the previous section, differences in bone structure were discussed, particularly differences in cortical and cancellous bone. Due to the microstructure of cortical bone, cortical bone is more stiff than cancellous bone, and fails at a lower strain. This makes anatomical reduction and compression of the fracture critical when promoting direct bone healing for repair of long bones of the appendicular skeleton. Cancellous bones are less stiff, sustaining greater strain before ultimate failure. The ribs are primarily composed of cancellous bone. *In vivo*, bone is subject to complex loading conditions that are difficult to replicate *in vitro*. *In vitro* mechanical testing of bone consists of load applied in compression, tension, bending, shear, or torsion. Bone is anisotropic which means that its mechanical behavior differs depending on the direction of the applied load. Bone is strongest in compression, weaker in shear, and weakest in tension. The applied load will produce fracture configurations according to the bone's mechanical properties with tension producing a transverse fracture, compression an oblique fracture, torsion a spiral fracture, and bending a slightly transverse fracture starting at the tensile surface of the bone and propagating toward the compression side, along shear planes resulting in a butterfly fragment on the compression surface. Mechanical testing of bone is performed by applying load in different directions and at different rates. Mechanical testing of bone allows the determination of the material and structural properties of bone. When testing material properties, a load-deformation curve is used (Figure 5). The load-deformation curve has deformation on the x-axis and load on the y-axis. The load-deformation curve is meant to be a visual map of how a material such as bone behaves when subjected to a force.[6] As load is applied to the bone, the bone will deform in response to the applied load. When load is first applied, the bone undergoes rapid deformation via fluid shifts within the bone matrix, as well as straightening of collagen and elastic fibers (toe region). As more load is applied, little deformation occurs further, producing a steep, linear slope that represents the stiffness of the bone. During this phase of testing, load is sustained by the innate strength of the bone components. The energy (defined as the area under the curve) that is stored during this phase of testing is known as elastic energy, because the load does not induce permanent deformation, meaning that if the load is removed, the bone will return to the bone's original shape. If load continues to be applied, the bone will reach a critical point, known as the yield point. It is at this point that the bone does not fail but is permanently deformed or changes shape with additional smaller loads, resulting in greater deformation, flattening the curve's slope. This phase of testing is known as plastic deformation, and the energy absorbed by the tested bone is known as plastic energy. Ultimate load occurs when the bone can no longer withstand any load, resulting in a downward turn of the curve (negative slope) or fracture of the bone. Load can be applied to a bone through bending, compression, tension, shear, torque, or a combination of these forces (bending, compression, tension, etc).

Equine fracture repair methods have been tested *in vitro* for strength, stiffness, and strain using various bending and compression mechanisms in a static and dynamic state. To understand fracture repair biomechanics, basic concepts regarding bone biomechanics must be understood. When load is applied to bone, the bone will deform in response to the applied load according to the bone's structural properties.[6] If the load applied to the bone is minimal, the bone will remain unchanged. With a mild to moderate amount of load, the bone will change shape when the load is being applied but can resume its normal shape with no structural change when the load is taken away. When the load applied to the bone is more than it can handle, deformation or a permanent change in shape can occur. If this load is continually applied, ultimate failure or fracture occurs.

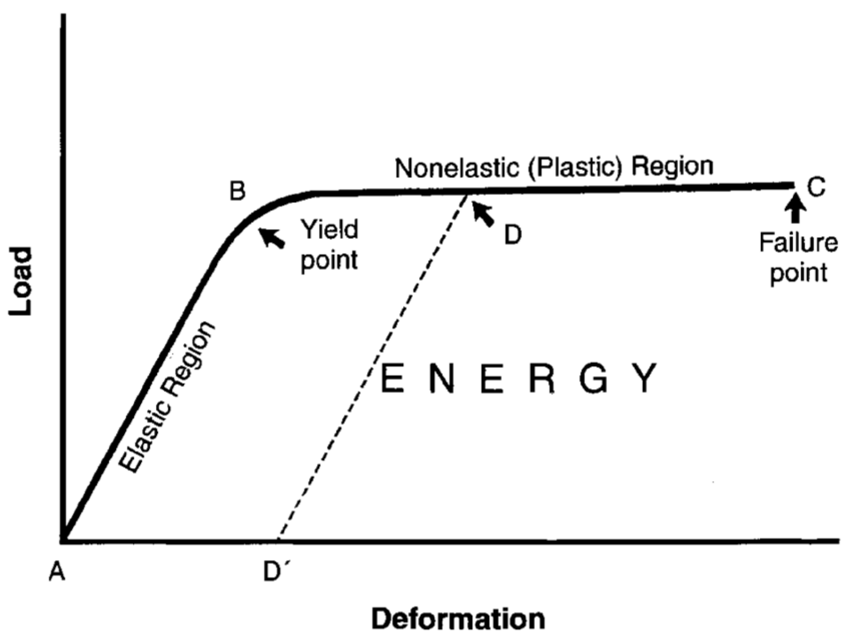

Figure 5 Load Deformation Curve. (Nordin, 2018)

Three important factors are recorded in a load deformation curve, including strength, stiffness, and energy absorbed. The strength is recorded as the ultimate load or force applied when the bone reaches failure or fracture. The stiffness is the amount of load before the bone reaches the yield point during the elastic region. The stiffness is calculated by dividing force by displacement. Energy absorbed is the amount of energy it takes for the bone to reach the ultimate failure point. This is calculated by measuring the area under the curve.[7,8] The load-deformation curve provides information regarding a bone's response to a force applied and can evaluate specific fracture configurations that can occur. This can then be translated to evaluation of fracture repair methods.[6] The load-deformation curve represents the mechanical behavior of the structure; however, it does not accurately evaluate the structure's composition and how this affects the mechanical behavior.[7,8]

Mechanical evaluation of the composition of the structure can be performed using a stress-strain curve. Stress is described as a force within a structure when an external load is applied. Strain is a change in dimension within a structure when an external load is applied. The load-deformation curve and the stress-strain curve are fundamental biomechanical tools used to evaluate how bones and orthopedic implants respond to physical forces, differing primarily in whether they measure a structural entity or a specific material. The load-deformation (or force-displacement) curve measures structural properties, capturing how a whole, intact bone—including its specific geometry, size, and density—behaves under an applied external force. In contrast, the stress-strain curve measures intrinsic material properties by normalizing force over area (stress) and change in length over original length (strain), effectively isolating the quality of the bone tissue itself regardless of its shape or size. This clinically allows researchers and orthopedic surgeons to distinguish whether a patient's bone vulnerability stems from structural defects (such as a thin cortical shell) or material degradation (such as the brittle, poorly mineralized bone matrix seen in severe osteoporosis).

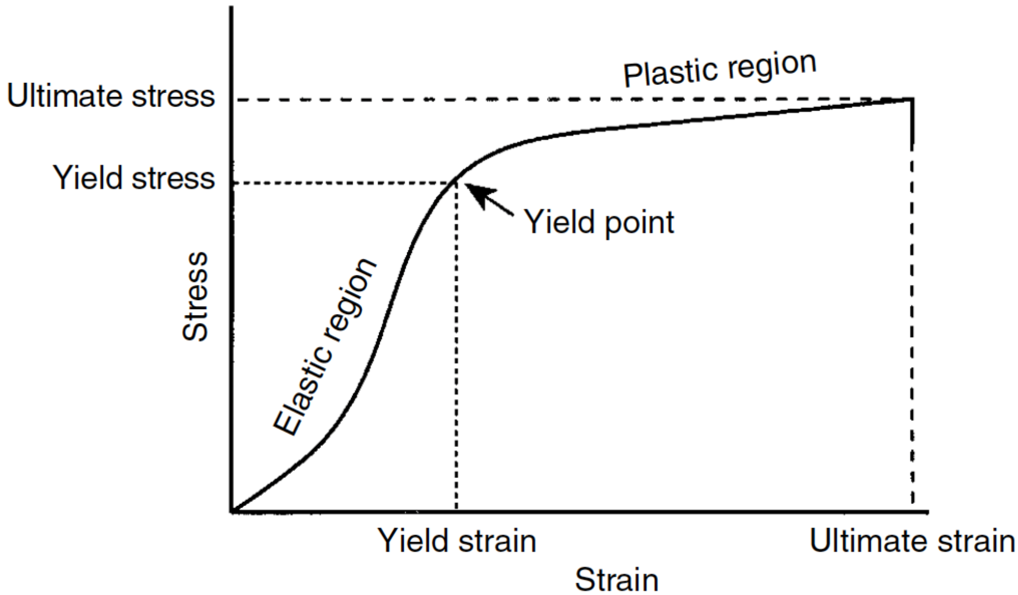

Figure 6 Stress-strain curve tested in compression. (Markel, 2019)

ii. Biomechanical Behavior

During normal daily activity, bone is subjected to forces in multiple directions producing tension, compression, bending, shear, and torsion.[6] Tension occurs when an equal traction load is applied to each end of a structure, lengthening and narrowing the structure in the process.[10] Fractures tend to occur in a transverse orientation when tension is applied. Bone is weakest on the side where tensile forces occur.[11] The opposite occurs with compression, as equal compressive forces are applied to opposite ends of the structure, causing it to shorten and expand radially.[10] Bone is strongest in compression, and pure compression fractures are rare in horses, for example cervical compression fractures in foals. Bending is a combination of tension on one side of the structure and compression on the opposite side of the structure. Experimentally, bending can be induced by either a three-point bending or four-point bending mechanism. The weakest side of the structure will be the tension side. Torsion occurs when load is applied to a structure, and it twists around a longitudinal axis. Bone has relatively low resistance to shear stress, whether applied parallel or perpendicular to the neutral axis, making it more susceptible to failure under shear loading. This can explain why, when a bone fails from torsional force, it initially breaks parallel to the neutral axis and then propagates along the tension stress, causing a spiral fracture to occur.[10] Combined forces are more common clinically and harder to replicate in an experimental setting.[11]

The biomechanical behavior of the equine rib under functional loading is governed by an asymmetrical distribution of stress, where the outer cortex predominantly acts as a tension surface, and the inner cortex acts as a compressive surface. Structurally, the horse rib is an elongated, curved cortical bone shell filled with trabecular bone, acting mechanically as a curved beam subjected to both axial loading from the thoracic sling and bending moments from respiratory muscle contractions. During deep inhalation or the impact phase of locomotion, muscular pulling forces and internal lung expansion force the rib to bend outward, placing the outer (lateral) surface under high tensile stress that pulls the bone matrix apart. Conversely, the inner (medial) surface faces inward-pushing, squeezing forces, placing it under high compressive stress. Microdamage or structural failure typically initiates on the outer tensile surface where the bone fibers are stretched beyond their mechanical limits, rather than the stronger inner compressive surface. This mechanical balance allows the rib cage to elastically deform and store energy during the repetitive gaits of the horse without suffering catastrophic fracture.

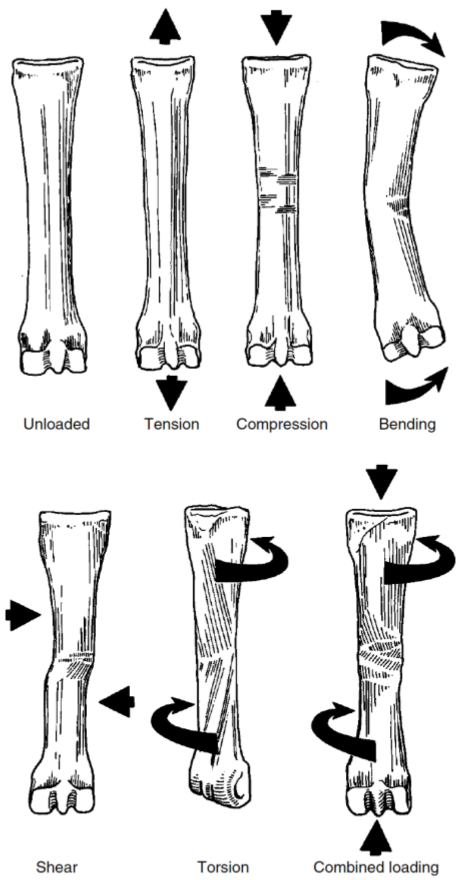

Figure 7 Loading of third metacarpal bone. (Markel, 2019)

There are numerous fracture fixation techniques available for different bone types and configurations. Selection of an appropriate fixation (or repair) method requires consideration of axial, bending, and torsional biomechanics, as most bones are subjected to combined loading. In equine patients, regional strain patterns within the bone help determine the optimal location and orientation of fixation. For example, a plate fixation for a fracture repair system should be applied on the tensile surface of a bone.[9] The fixation systems are then tested under certain conditions to prove their strength and stiffness compared to that of the intact bone before fixation.

iii. Three-Point and Four-Point Bending

Use of a three-point bending mechanism is a widely used testing method for various materials, providing measurements of Young's modulus of elasticity (E) or stiffness of a material, and the tensile strength of the material. In three-point bending the material is under the same amount of tension versus compression, and the material fails or fractures due to tension not shear, as in other types of compression testing.[12] The three-point bending test has two supports the test material rests on, and one point of deflection centered on the opposite side on which the force is applied(Figure 8). Due to this one point of deflection, there is high stress concentration at a single point on the bone, which can be useful when creating a fracture line. By concentrating the maximum bending moment directly under a single central loading nose, the test forces a predictable fracture at the midpoint, making it ideal for measuring the mechanical properties of a targeted local section.

The four-point bending test differs in that there are two points opposite the supports that force is applied(Figure 8). The two points spread the region of stress such that a larger portion of the material is tested with force compared to the three-point configuration.[13] In four-point bending, the loading nodes or deflection points must be centered and a predetermined distance away from the two supports to maintain low shear strength and high tensile strength. The four-point bending is the current gold standard for *in vitro* testing of surgical implants when determination of strength and stiffness is the determinants of interest.

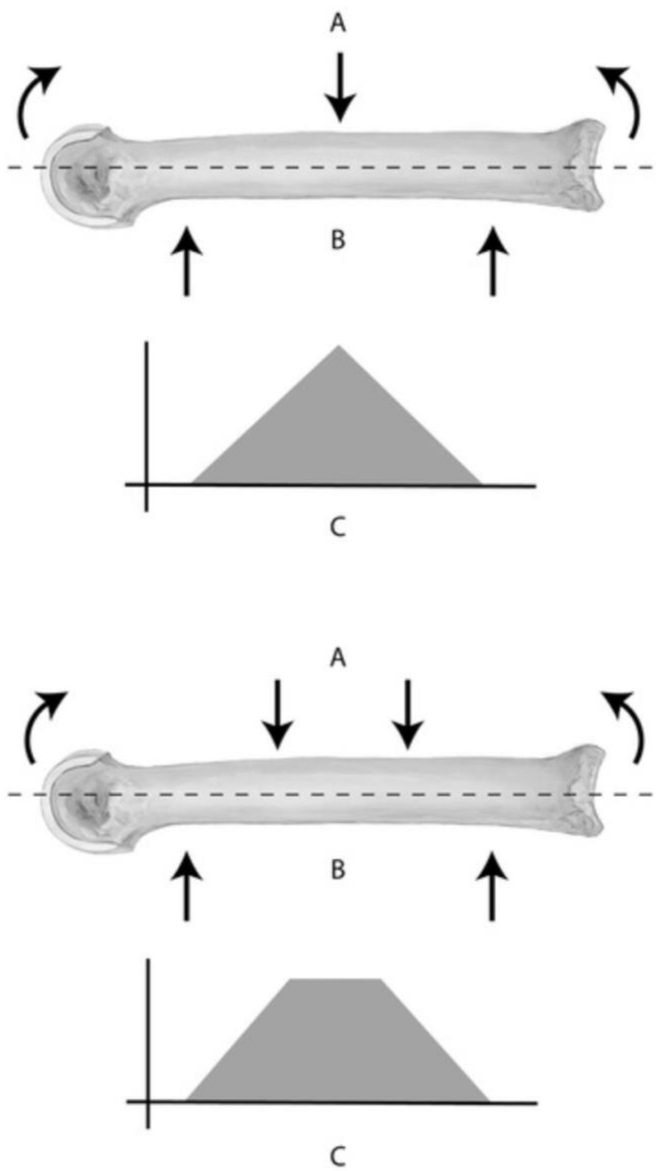

Figure 8 Three-point and four-point bending. (Auer, 2018)

iv. Axial Compression

Axial compression testing is a mechanical evaluation method where a crushing force is applied directly along the longitudinal axis of a sample to measure its structural strength under load. During the test, a mechanical ram pushes down on a specimen at a controlled rate until it deforms and ultimately fails. Axial compression testing is another widely used technique to determine mechanical properties of bone. Measurements such as elastic modulus and ultimate strength can be produced easily.[20] Elastic modulus is a quantitative measure of a material's resistance to elastic deformation when a stress is applied . Currently, there is not a standardized method to perform compression testing of human bone due to the differences in biological tissue, gripping bone surfaces, and low loads that have been applied. Stiffness has been difficult to accurately compare between studies due to patient demographics, location, orientation, and testing conditions. Zhao et al, discussed these variances and created methods to standardize a protocol for obtaining stiffness values that can be compared.

Accurately determining the elastic modulus depends on critical experimental parameters, including precise anatomical alignment and the use of fresh, hydrated specimens stored in physiological saline; notably, allowing specimens to dry prematurely significantly increases material stiffness. To calculate a value closest to the true elastic modulus, researchers recommend fitting a best-fit line to the steepest portion of the linear stress-strain curve across a tight 0.2% strain interval. Restricting the evaluation to a range below this 0.2% threshold ensures that confounding plastic deformation remains minimal within the calculation.[21]

Axial compression testing is typically recommended for evaluating skeletal structures that experience physiological weight-bearing loads along their longitudinal axis, such as the vertebrae and lower limb bones. For bones that are irregularly shaped, or contain a trabecular pattern, axial compression is often inadequate due to the adjustment for cross-sectional area. Often, placing these specimens in this axial compression manner, errors can easily occur due to bone slippage or variances in placing an irregularly shaped bone within the testing device.[22] Since bone is strongest in compression, fracture fixation methods target supporting of tension, bending, and torsional forces. Testing an implant with the use of compression methods can make the implant look falsely stable due to each fractured end sharing the load.

Figure 9 Axial compression testing of a human rib. (Mischler, 2022)

C. Human rib fracture biomechanics

i. Breathing Mechanics

Over the past 20 years, there has been increased interest in managing chest wall injury in humans with an emphasis on early restoration of chest wall stability to reduce pain and pulmonary complications in patients. SSRF has been shown to provide better pain control while restoring respiratory function, reducing patient mortality, and reducing ICU and hospital length of stay, minimizing costs, and enabling an earlier return to daily activities with an improved quality of life compared to conservative management.[57,58] SSRF is recommended within < 48-72 hours of injury when the patient has intractable pain due to rib fracture, chest wall instability, and/or needs respiratory support.[58]

In adult humans, previous recommendations for the management of flail chest injuries were mechanical ventilation with minimal cases undergoing internal fixation. Mechanical ventilation has high rates of complications including pneumonia, sepsis, and acute respiratory distress syndrome. Malunion or non-union with indirect fracture healing can occur and decrease the long-term quality of life for the patient.[14] More recently, evidence suggests that internal fixation can decrease the morbidity and mortality associated with adult rib fractures.. A recent human biomechanical study compared intact, fractured, and fixated ribs to demonstrate normal rib biomechanics and the effects of a fracture or fixated rib on this model.[14]

Myers et al used a previously validated human breathing model describing the angular kinematics of the costovertebral joints during respiration. The degree of motion of the rib cage during the act of breathing in a standard adult human was defined.[15] Using this breathing model, they re-created the forces in various directions on the rib cage. In all axis of motion, the results indicated fractured ribs significantly increase interfragmentary motion at both fracture ends altering the biomechanics of the chest wall. Whereas the fixated ribs decreased the interfragmentary motion seen with fractured unrepaired ribs, and preventing inward motion that inspiration could cause.[14]

These study results objectively support CT images showing increased lung volumes of adult humans after fixating flail chest when compared to pre-operative images with lower lung volume.[16]

ii. Surgical versus medical management in adults

A recent systematic review and meta-analysis was performed regarding the clinical outcome in patients treated with surgical versus conservative methods. Over one million patients were included in this study, and the factors of how many ribs were involved, age of patient, length of hospital stay, cost of stay, duration of mechanical ventilation, and mortality were analyzed. Patients who received surgical stabilization of the rib fracture(s) (SSRF) overall had a lower mortality rate and better outcomes. Patients undergoing SSRF within 72 hours had a shorter length of hospital stay, however over 72 hours had a longer length of hospital stay than conservative treatment. Healthcare costs were increased with SSRF; however, the duration of mechanical ventilation was decreased with SSRF. The study concluded that patients with multiple rib fractures, including flail chest, treated with SSRF had a lower mortality rate. It is recommended to repair flail chests in the acute phase, especially in patients over 60 years old.[17]

According to the 2025 Chest Wall Injury Society (CWIS) consensus guidelines published by Bauman et al. in the Journal of Trauma and Acute Care Surgery, SSRF is primarily indicated for patients with objective chest wall instability, including flail chest and severely offset fractures (≥3 ipsilateral ribs with 100% displacement). Secondary indications include failure to wean from mechanical ventilation within 48 hours due to rib fracture pain and, in non-ventilated patients, persistent, severe respiratory dysfunction (e.g., incentive spirometry <50% of predicted) despite multi-modal analgesia.

a. Pediatric rib fracture

Pediatric rib fractures are significantly less common than adult rib fractures. This is most likely due to the cartilaginous flexibility of a neonatal rib versus the adult rib where osteoporosis can be underlying. In infants, rib fractures are commonly due to non-accidental injury, with birthing trauma accounting for less than 8% of infants with rib fractures.[56] SSRF of the infant or even pediatric patients is often not pursued due to concern for disruption of normal rib growth and subsequent asymmetry of the chest wall. There are limited studies of pediatric rib fractures and establishment of best practices. A recent case series by Kessel et al. (2014) reported on 328 children with one or more fractured ribs, aged 0-14 years old. Most of these ribs were fractured due to accidental trauma, such as motor vehicle accidents. Children had a lower number of fractured ribs, but increased rates of extra-thoracic injuries with similar mortality rates.[18] Polycarpou and Kim (2021) demonstrates that SSRF is a safe and feasible intervention in pediatric patients. Key indications for SSRF in young, severe trauma cases include prolonged mechanical ventilator dependence, significant chest wall deformity, and intractable pain that hampers respiratory effort. The literature regarding pediatric surgical stabilization includes children from ages 6-16 years, but repair of fractured ribs in children less than 1 year of age has not been reported.[19]

iii. Biomechanical testing on current fixation methods

a. Advantages and Disadvantages to current fixation systems

The primary goal of SSRFcommonly known as rib plating—is to restore the anatomical integrity and mechanical stability of the chest wall following severe thoracic trauma. By surgically realigning and secure-fixing displaced or flail rib segments with specialized titanium plates and screws, the procedure eliminates the painful, abnormal paradox motion of the chest wall during respiration. This rigid internal stabilization dramatically improves pulmonary ventilation mechanics, minimizes severe mechanical pain, and protects the underlying lungs and intercostal neurovascular structures from ongoing tissue trauma. Clinically, achieving these structural fixes enables patients to breathe deeply and effectively, which directly serves to accelerate weaning from mechanical ventilators, reduce intensive care unit (ICU) lengths of stay, and lower the incidence of life-threatening respiratory complications like pneumonia.

Plate system with screw fixation

Recently rib specific fixation systems have been developed that are anatomically designed to contour the external or internal shape of the rib. The MatrixRIB (Synthes GmbH) system is one of the most used plate and screw fixation systems currently being utilized in human SSRF. The locking plate system is applied with 2-3 locking screws on either side of the fracture using bi-cortical purchase.[24] This plate locking system was compared with the RibLoc and RibFixBlu locking plate systems by Prins et al. The MatrixRIB was found to be stiffer than the RibLox and RibFixBlu, but less stiff than intact adult rib. This biomechanical study revealed that the MatrixRIB mostly failed at the anterior drill hole, while the other two plate fixation systems failed at the most anterior drill hole or end of the plate.[25] Locking plate systems are being utilized for SSRF versus dynamic compression plates due to three major reasons. The adult human bone is osteoporotic and locking plates do not rely on bone rigidity; the stability of the locking plate relies on the fixed-angle construct instead of the bone-to-plate contact, and the locking plate conserves blood supply by preserving the periosteum.

Plating with Clip

Clip devices have also been used to stabilize adult rib fractures. These fixation systems wrap the ribs superiorly and inferiorly. Small staples are clamped onto each side of the rib to fixate the plate to the rib. The most common device being utilized is the STRACOS™ (MedXpert GmbH) system which is a titanium system that comes in various lengths pending the length of the rib. Unlike the locking plate systems, they are not contoured to the ribs, however they were only designed for rib fixation.[24] Prins et al tested the STRACOS system and found that it was significantly less stiff than locking plate systems. A less stiff construct may be more advantageous due to the dynamic movement of the thorax, and flexibility won't restrict natural movement. The modes of failure included: new fracture at the anterior portion of the implant, new fracture at the plate end, and plate deformation at the original fracture site.[25] The clip devices have many advantages including; the lack of screws needed when there may be poor bone quality, reduced operative time, and a more flexible construct.

The clip fixators and locking plate systems are currently the most widely used systems, although clinical reports of other fixations utilized include intramedullary fixation, bioabsorbable plates, and suturing techniques.[24] There currently is no evidence explaining the advantages and disadvantages to each of these systems.[24] However, the biomechanical study by Prins et al., discusses the benefits of rigid versus non-rigid fixation systems. Rigid fixation systems are stiff enough to decrease the interfragmentary strain while restoring pulmonary function, however, too stiff of a construct may impede respiratory mechanics immediately post-operatively or cause new fractures at the end of the implant. In adult humans, chest tightness and irritation are the chief complaints leading to implant removal. The locking plate system within the study had a higher stiffness on an intact rib than an intact rib without the plate system. They hypothesized this increased stiffness could be the cause of these subjective patient complaints. The clip fixators are less rigid and may be a preferred option for long-term fractures with simple configurations.[25]

D. Diagnosing rib fractures in equine neonates

i. Physical Examination

Foals with a history of dystocia needing manual obstetrical assistance, as well as those born to primiparous mares, are at increased risk for rib fractures and typically are presented between 1 and 3 days of age.[26] Upon clinical presentation, initially a brief physical examination is performed standing, if the foal can stand on its own. The respiratory rate and effort are assessed; signs of mild tachypnea or dyspnea to severe respiratory distress can be associated with rib fractures.[27] If a flail chest is present, where the segment of broken ribs sinks inward during inspiration and protrudes during expiration, immediate action for additional diagnostics and treatment is recommended, as normal breathing biomechanics has been compromised. If the brief evaluation while standing is normal, it is recommended to perform a physical exam and diagnostics in lateral recumbency. In dorsal and lateral recumbency, asymmetrical depressions may be evident, and abnormalities may include edema, pain upon palpation, and crepitus.[28,29].

In performing a standing physical examination, approximately 90% of foals with thoracic trauma can be identified on palpation and accurately diagnosed based on clinical suspicion. Whereas, dorsal recumbency a mild, moderate, and severe depression was in the cranioventral region present at the costochondral junction in 98% of foals with suspected thoracic trauma.[26] These foals were admitted for reasons unrelated to thoracic trauma. In dorsal recumbency, 69% of foals examined had unilateral mild or moderate thoracic depression visualized at or near the costochondral junction. However, the foals with thoracic symmetry palpated while in dorsal recumbency, 75% were diagnosed with rib fractures using ultrasound.[28] Physical examination may not diagnose every neonatal rib fracture, but foals with severe systemic abnormalities such as hemothorax or pneumothorax that may need to be treated before or during general anesthesia of rib repair, can be promptly addressed utilizing ultrasound to define the secondary complications more clearly.

ii. Radiography

After a thorough physical examination, additional diagnostics are then performed either with the foal in lateral recumbency or standing. Commonly, both right and left lateral and dorsoventral views are taken to locate rib fractures and other pulmonary lesions. Radiographs are sensitive for diagnosing severely displaced fractures.[28]

Definitive diagnosis for most long bone fractures is obtained via radiography.[30] Radiographs are a standard diagnostic tool for use in bone pathology, however, due to the nature of radiographs as a two-dimensional image of three-dimensional structures and marked superimposition of soft tissue within the thorax, subtle changes to the rib can be missed. Ultrasound has proven more useful in screening and diagnosing foals with rib fractures. Foal rib fractures occur most commonly just proximal to or at the costochondral junction, where radiographic interpretation may be difficult and insensitive for the identification of costal abnormalities as compared to ultrasonography. When these imaging modalities are compared, rib fracture(s) were identified in a majority of foals using ultrasound, but only few foals when radiographed.[28] The current gold standard for antemortem diagnosis of rib fracture is ultrasonography. This holds true in other species, with 78% of humans with rib fractures diagnosed with ultrasound, but only 12% were diagnosed with radiographs.[31] When diagnosing rib fractures and determining their location, it is important to assess for pneumothorax, which can result from a displaced, sharp rib fragment. Radiographic changes supportive of a pneumothorax include retraction of the normal pulmonary parenchyma and the dorsal margin of the lung lobes below the thoracic vertebral bodies.[32] A recent study showed increased sensitivity of ultrasound in diagnosing an experimentally induced pneumothorax compared to radiographs in healthy horses.[32]

iii. Ultrasonography

When the foal is in lateral recumbency, the thorax can be more thoroughly assessed from the costovertebral to the costosternal junctions, without additional movement, something that can be challenging in a restrained, standing foal. When performing an ultrasound of the rib, a high frequency ultrasound transducer is placed directly on top of the rib looking for incongruency of the surface, and/or hypoechoic fluid surrounding the rib.[33] Ultrasound is four times more likely to diagnose the presence, location, and degree of displacement of a rib fracture than radiography. In addition, ultrasound is better to evaluate the soft bone present along the costochondral junction and detect abnormalities than radiography.[28]

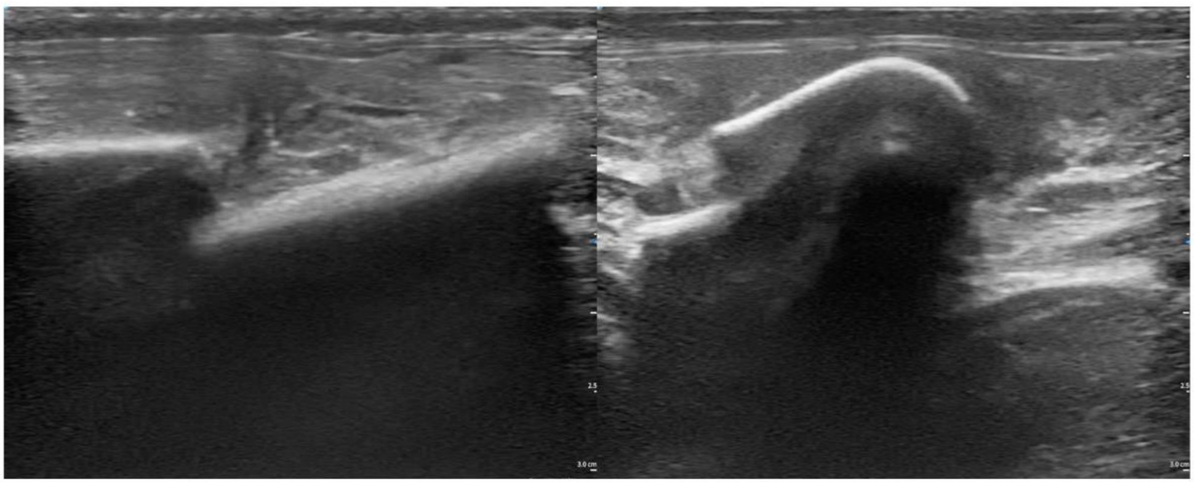

A B

Figure 10 A Ultrasound of rib fracture in longitudinal view and B transverse view. (Courtesy of Dr. Matt Coleridge)

Detection of pneumothorax in the foal can also be performed using ultrasound while concurrently evaluating for rib fractures and abnormalities of pulmonary parenchyma. Absence of a movement of the hyperechoic visceral pleural line (or absence of a "glide sign") is an indication there may be air in the thoracic cavity. Ultrasound is considered more sensitive for diagnosing a pneumothorax and evaluation of pleural pulmonary abnormalities compared to radiography.[32] The gold standard for evaluating pneumothorax and rib fractures for both human and foals was historically radiography, however recent literature suggests there is a higher sensitivity for both soft tissue and bone abnormalities when using an ultrasound when compared to radiography.

iv. Computed Tomography

Ultrasound is initially used to confirm the rib fractures in equine neonates. However, ultrasound requires systematic evaluation of each rib leaving room for missed pathology due to the inability to evaluate the entirety of the thoracic cavity. In human medicine, patients with thoracic trauma and suspected rib fracture are subject to advanced imaging using computed tomography (CT). In human medicine this has become the gold standard for identifying fracture location, number, displacement, and comminution of rib fracture as well as identification of underlying pathology within the thoracic cavity including pulmonary contusion injury.[34] Computed tomography (CT) has become more readily available in equine practice, proving useful in the diagnosis of rib fracture. CT may be performed under injectable anesthesia, eliminating motion that can prove difficult in ultrasound or radiographic examination while allowing enhanced visualization of the more cranial ribs that are difficult to image due to the humerus and surrounding soft tissues.[35]

The use of the CT for neonatal equine rib fractures more accurately identifies the exact location of cranial rib fractures, which is recommended for planning of surgical fixation. One study in which foals were either diagnosed with rib fracture using ultrasound, CT, or both prior to surgery, reported disagreement in presence, degree of displacement and fragmentation of rib fracture in 76% of cases.[35] All ribs in this study were repaired with securos ® suture in a figure eight pattern. Total anesthesia time differed by approximately 10 minutes in the CT group. Post-operatively, 62% of non-survivors were diagnosed with rib fracture by ultrasound alone, and on necropsy were discovered to have fatal pericardial pathology. This was presumed due to undiagnosed and untreated cranial rib fractures. This study highlights the importance of advanced imaging to aid proper identification of rib fracture and underlying thoracic pathology for pre-operative assessment and surgical planning.[35]

Using a CT as a diagnostic tool has only been performed and evaluated as a preoperative surgical tool rather than a diagnostic for foals that may only require medical management in rib fracture cases. Garrett et al discusses the use of CT for preoperative planning. It is currently not recommended that CT replace the use of ultrasonography due to both medical (general anesthesia) and financial reasons. The use of ultrasonography is currently recommended as a first line diagnostic in equine neonatal rib fracture and to decipher if they are a candidate for surgical repair or can be treated with conservative management.[35]

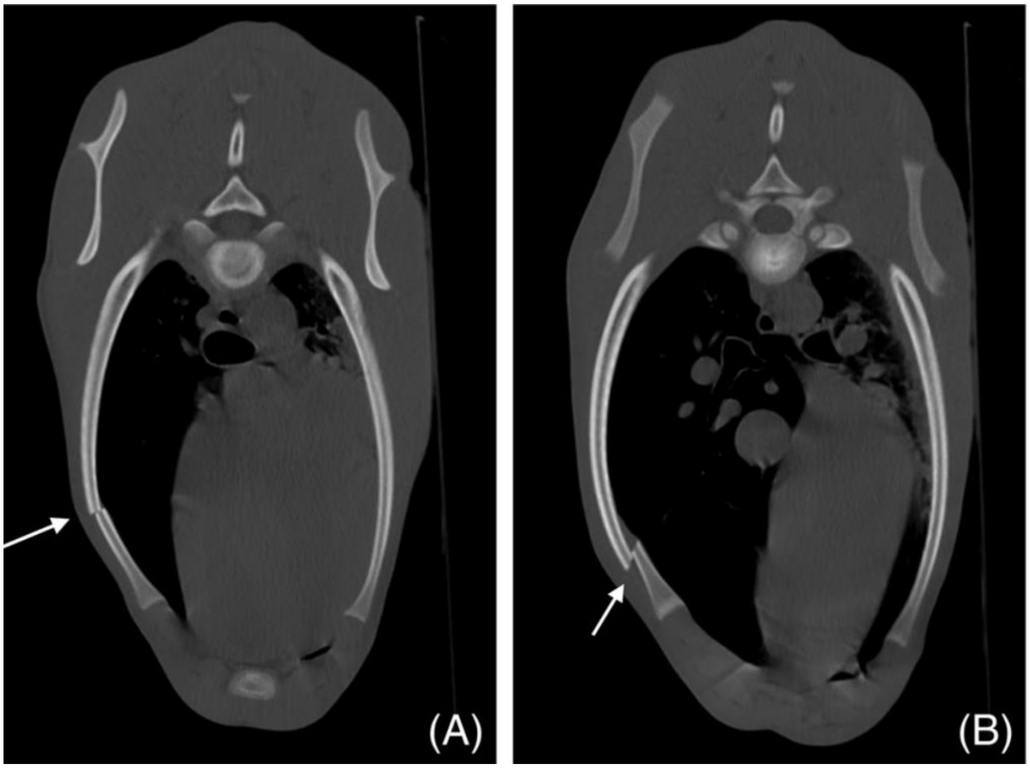

Figure 11 Fractured equine neonatal rib using CT A minimally displaced rib and B displaced rib fracture. (Garrett, 2022)

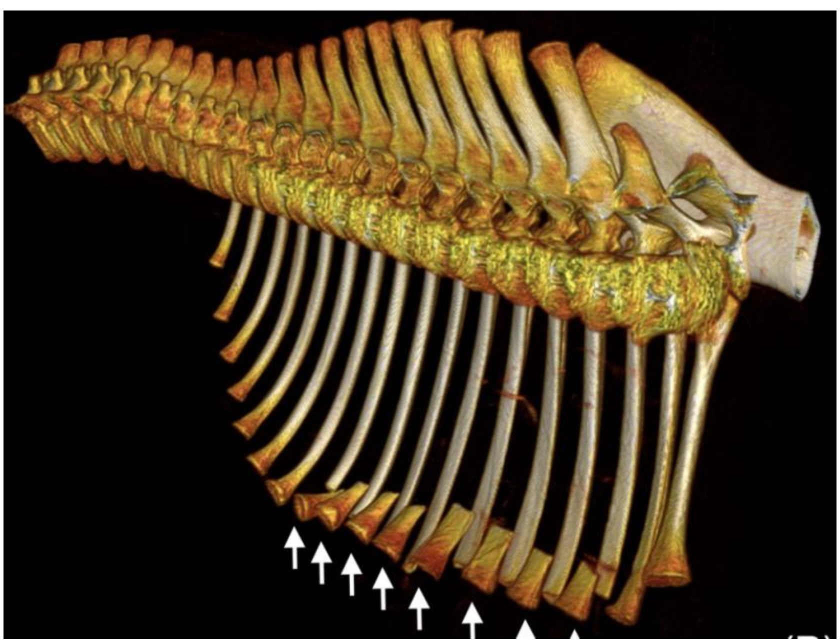

Figure 12 Three-dimensional view of CT equine neonatal rib fractures. (Garrett, 2022)

E. Current management of equine neonatal rib fractures

i. Conservative Management

Conservative management for the treatment of neonatal rib fractures in horses is recommended when no vital structures have been injured, and there is limited potential for vital structures to be harmed.[29] The preferred management is stall rest and supportive care as needed. Stall rest for foals can be a difficult option as both the foal and mare need to be considered. Mares may require a sedative for the rest period, however, oral sedatives are generally not recommended for foals. Exercise restriction in foals is not recommended for prolonged periods of time due to the potential for acquired flexural and angular limb deformities. Excessive rich nutrition of a nursing foal while on stall rest is common and can be a contributing factor to these deformities.[36] It has been recently proposed that early exercise for a foal can lead to increased performance later in life.[37] This literature supports less time on exercise restriction.

A recent human study compared conservative management to surgical stabilization and concluded early stabilization decreases pain, complications, and periods of required rest.[38] Pain in neonatal foals is hard to grade, with the basic understanding if they are nursing and no lameness is visualized, it may go undiagnosed. Recent literature has created a model for grading acute pain in foals by their facial expressions with good to excellent intra-observer agreement, however a limitation to this study was the low number of patients and the differences in breed and biological sex.[39] On large breeding farms it has been reported approximately 20% of foals can have thoracic trauma including either rib fractures or costochondral junction dislocation, and following these foals there was no clinical problems associated within a 6-month period.[26] This suggests a large number of non-displaced rib fractures may go undiagnosed and heal on their own without exercise restriction.

ii. Fracture Fixation

Fracture fixation is indicated if vital structures have been injured or there is a potential for vital structures to be injured.[29] There are a variety of fixation techniques including rigid versus non-rigid fixation that are currently being used. In all techniques discussed in this section, foals are placed under general anesthesia in the opposite laterality of the repaired fractured rib. An incision was made for repair of cranial ribs through the skin, incising through the serratus ventralis musculature. For the more caudally repaired ribs, the incision was made through the cutaneous trunci muscle down to the periosteum. Two rib fractures are commonly repaired through one incision. A two-layer closure is performed thereafter, apposing the muscle and skin. [27,29,40-42]

a. Nylon Suture

A Securos Cranial Cruciate Ligament Repair System (SCCLRS) has been commonly utilized as an extracapsular stabilization method for treating canine stifle injuries. This system utilizes the 80-pound nylon suture. In 2005 a case report was performed utilizing this repair method, reporting it as an effective method.[41] The foal in this case was a 3-day old Standardbred colt which presented within 24 hours of birth. The foal did not respond to medical management of 6 cranially displaced rib fractures and all ribs were repaired using the SCCLRS system. Noted benefits of the system were the secure stabilization with rapid application, requiring approximately 20 minutes per rib for repair.[41] Survival to discharge was reported in this foal, highlighting this as a possible repair strategy for rib repair.

When repairing with the SCCLRS system the dorsal and ventral segments are generally reduced using the application of towel clamps and a 2.5mm drill bit is used to drill a hole from the dorsal or ventral end exiting the abaxial surface at the cranial border approximately 1.5cm ventral to the fracture, on both the dorsal and ventral fracture segments. The 80-pound strand of nylon is then passed through these holes in a figure-of-eight pattern in which the free ends are tied dorsal to fracture plane. With the SCCLRS technique, there are three areas where clamps are required for the tensioning device. One placed with the caudal strand going cranial and the cranial strand going caudal and then two additional clamps on each strand. Once the reduction is complete, the tensioning device is applied to the crimped clamps, and the nylon strands are tightened.[40]

Modifications to this technique have been made for calf neonates since the ribs are flatter and more cartilaginous. The holes may be created with a 2mm diameter Steinmann pin and Jacobs chuck and applying the nylon suture in a cruciate pattern.[43] Another option in a calf or a small foal with narrow ribs is drilling two holes in each fragment from the abaxial surface to the axial surface cranially and caudally and placing the figure eight strands on the axial side of the fracture. Other variations of large diameter non-absorbable suture include FiberWire ® or Ethibond ®. These variations may be more cost effective, however the strength and tightening ability may be variable.[40]

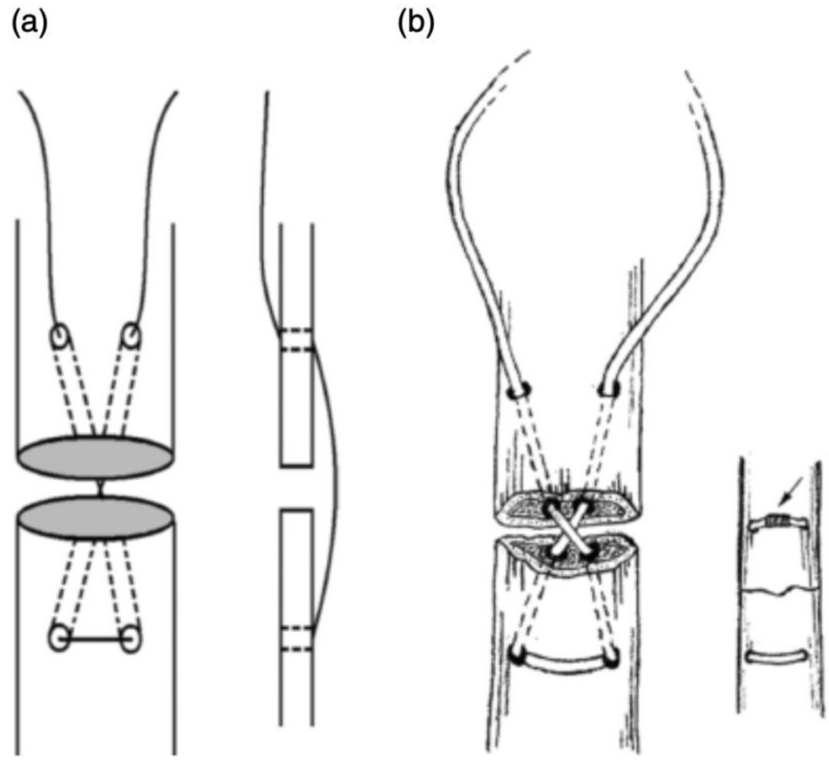

Figure 13 Nylon suture A modified technique axial to rib B original technique. (Levine, 2022)

b. Nylon Cable Tie

Use of a nylon cable tie (NCT) was first introduced using the same technique of fracture reduction with the use of a towel clamp as stated above with the SCCLRS technique. Based on rib width, either a 3.2mm, 4.0mm, or 4.5mm drill bit is utilized to create a drill hole approximately 5-10mm dorsal or ventral to the fracture line on both fracture fragments. For the larger drill holes, a 4mm wide gas sterilized nylon cable tie was placed and the smaller hole a 2mm wide and 10-16mm long NCT. The NCT is placed through the drill holes with the tightening apparatus on the abaxial side of the fracture line with the use of needle drivers or hemostats. When appropriate reduction was achieved, the NCT was tightened and the free end trimmed close to the lock.[42] This technique was modified due to displacement of the fractured ends and puncture of this displaced end into the pericardium ending in death.[44]

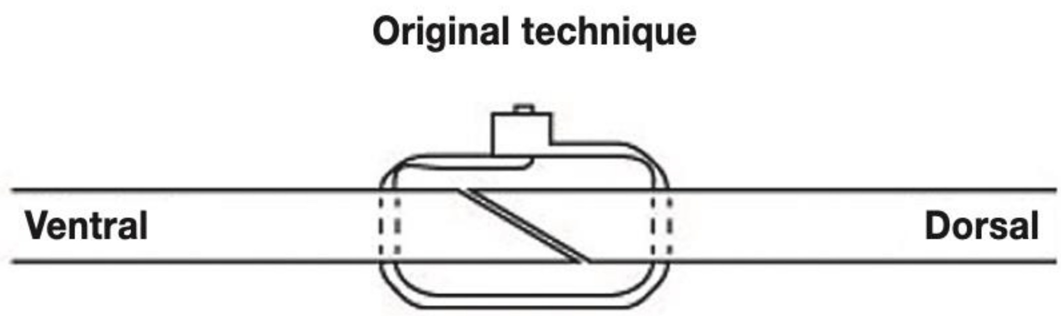

Figure 14 Original nylon cable tie technique. (Williams, 2013)

The modified technique was reported by the same surgeon as the original technique described. In both techniques, the ventral fracture fragment was overriding the dorsal fragment in most fractured ribs. In the modified technique, the fracture was not reduced and left in this overriding manner. In the original technique, the NCT was placed longitudinal to the rib; however, in the modified technique, the NCT was placed in a transverse fashion on the cranial aspect of the fractured ends. The cranial edge was chosen to avoid the neurovascular bundle at the caudal edge of each rib. The NCT was then tightened, locking the fractured non-reduced ends together, and the lock was then trimmed.[44]

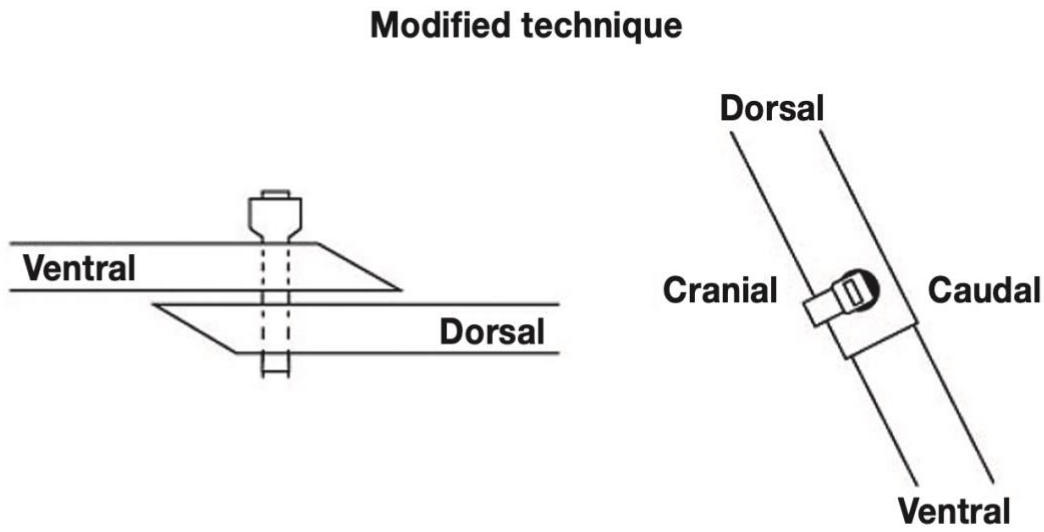

Figure 15 Modified technique using a nylon cable tie. (Williams, 2013)

c. Modified reconstruction plate

A 2.7mm reconstruction plate is a good size to appropriately fit the surface of equine neonate cranioventral ribs. A larger size, for example, the 3.5mm reconstruction plate is too wide for the width of a neonate rib and would cause impingement on surrounding soft tissues. However, the larger screw diameter of the 3.5mm would be of benefit as there would be more bone purchase. For these reasons the 2.7mm reconstruction plate was modified to fit a 3.5mm cortical screw using a 3.2mm drill bit to manually ream the holes. The modified plate is then contoured to fit the rib, and a 2.5mm drill bit is then utilized to create thread holes in bi-cortical fashion. Approximately 2-3, 3.5mm self-tapping cortical screws are then placed both proximally and distally to the fracture line. The length varies from 10-14mm; however, it has been reported that 14mm in length may be too long and therefore disrupt underlying vital structures. In most cases, a 5USP cerclage wire is then placed surrounding the rib and implant proximal and distal to the fracture line to provide additional stability. It has been the author's experience surgeons are moving away from the use of Backhaus towel clamps and instead using the cerclage wire to appose the fragments before implant application. This negates the potential for a stress riser to occur from the towel clamp on a smaller fragile rib fragment.[27]

Figure 16 2.7mm modified reconstruction plate with cerclage wires placed proximal and distal to fracture line. (Courtesy of Matt Coleridge)

This chapter establishes a comprehensive framework for equine neonatal rib fracture management by linking fundamental bone biology, such as healing mechanisms and ossification, with mechanical principles like load-deformation curves and bending, and evaluating diagnostic methods including ultrasonography and CT. It further analyzes human clinical outcomes, specifically comparing medical and surgical interventions, to evaluate current equine fixation techniques.

Chapter 2 Objective

The objective of this study was to evaluate the biomechanical properties of intact and repaired equine neonatal ribs using four different methods of fracture fixation.

i. Hypotheses

We hypothesized that rigid fixation (modified reconstruction plate and SOP) would result in stronger and stiffer repair constructs than non-rigid fixation (NCT and RC). Additionally, we hypothesized that the nylon cable tie and rib clip would fail most commonly at the original fracture.

Chapter 3 Materials and Methods

i. Study Design

Neonatal foals submitted for diagnostic postmortem examination to the University of Kentucky Veterinary Diagnostic Laboratory for reasons other than thoracic trauma were used for the study. Foals were included if they were less than 2 weeks of age. Specimens were excluded if, on necropsy at University of Kentucky Veterinary Diagnostic Laboratory, there was evidence of thoracic trauma acquired during birth or thereafter. Signalment and total bodyweight were recorded for each specimen, as well as reasons for euthanasia or death. Both the left and right rib cages were harvested, wrapped in moistened towels, and stored at -80°C until testing. For each thorax, bilateral ribs 3 to 6 ribs were selected for fixation due to the current recommendation of SSRF in this cranial thoracic region. Sample size was obtained by performing a priori power analysis using G*Power (Heinrich-Heine-Universität Düsseldorf, Düsseldorf, Germany). A significance threshold (α) of 0.05 and power (1-ß) of 0.80 were assumed, as well as 2-sided tests. A paired t-test was used as a surrogate for the linear mixed model analysis and scaled up for 4 groups. A mean increase from control of 100 N for yield load with a standard deviation of 189, and a low correlation (r=0.4) extrapolated from human data resulted in a sample size of 20 ribs/group requiring a total of 10 foal cadavers.

Each rib was randomly allocated to one of four repair groups: 4mm Nylon Cable tie (industrial grade polyamide 6.6) (NCT), a modified 2.7mm AO reconstruction plate manually reamed to accommodate 3.5 cortical screws referred to as a modified reconstruction plate (Vet ovation Raleigh, North Carolina) (MRP), 2.7 mm string of pearls locking plate (Vet ovation Raleigh, North Carolina) (SOP), and STRACOS™ Titanium 3D rib clip (MedX- pert GmbH, Eschbach, Germany) (RC). Due to the number of variables including ribs tested, side (L or R) of thorax, and repair group, equal distribution of all variables within each horse was not possible. Each rib, considering the side of the thorax from which it was obtained, was randomly allocated to ensure equal representation of all variables within each repair group.

ii.Biomechanical testing and fracture of intact ribs

At the time of testing, each rib cage was thawed overnight at room temperature. Ribs 3-6 were disarticulated from the vertebrae, and all surrounding soft tissue, including the intercostal musculature, was removed. Measurements of length, height, width, and circumference of each rib were obtained and recorded by the same investigator (KN). Each intact rib was subjected to a single-cycle to failure three-point bending test. The force was applied to the extra-thoracic, concave surface of the rib to simulate external trauma that would be sustained during dystocia, creating a simple, transverse fracture at approximately 50% of the rib length. For all three-point bending tests, the force was applied with a crosshead speed of 0.25mm/s at a loading distance of 35 mm and support span distance of 90 mm using the Instron 5565 universal materials testing machine (Instron, Norwood, Massachusetts) (Figure 1 a and b). The support span and loading distance were selected to suit all size variations of the tested rib numbers and cadavers. All specimens were loaded to failure, and the maximum force reached (F_{max}) and force at failure (F_{fail}) recorded.

iii. Repair of fractured ribs

Ribs were then repaired according to their assigned repair group. All repairs were performed by the same investigator (KN). Figure 17 shows an example of the final repaired construct for each group.

For the NCT repair group, a 3.2 mm drill bit was used to drill a central hole 5 mm from the fracture line for both the proximal and distal fragment. Then a 4 mm wide, 406 mm long nylon cable tie was threaded through the drill holes in a parallel orientation to the rib and manually tightened opposing the fracture fragments and reducing the fracture. The excess cable tie was removed close to the lock.

For the modified reconstruction plate (MRP) repair group, a 2.7mm 26-hole AO reconstruction plate was manually cut into 20, 6-hole plates and then manually reamed with a 3.2 mm bit to accommodate 3.5 mm cortical screws as previously described.[45] The fracture was reduced; the plate was contoured if needed, and a bi-cortical thread hole was drilled using the 2.5 mm drill bit through each plate hole. Six, 3.5 mm cortical self-tapping screws, 12mm in length, were placed and tightened by hand. Two pieces 5 USP cerclage wire was then placed around the rib and plate, proximal and distal to the fracture line, between the first and second screws and fifth and sixth screws. The wire was tightened using orthopedic wire twisters with excess wire removed.

For the SOP repair group, a 2.7 mm 20-hole SOP plate was manually cut into 20, 6-pearl plates. To repair the fracture, the fracture was reduced, the plate was contoured if needed, and a bicortical thread hole was drilled in the center of the pearl using a 2.0 mm drill bit with a 2.7 mm drill guide. Six, 2.7 mm cortical self-tapping screws 12 mm in length were placed into each drill hole and tightened manually.

For the RC repair group, STRACOS™ Titanium 3D rib clips (Medxpert, Deutschland, Germany) 21 mm in width were cut into 20, 6-prong segments. The fracture was reduced, and the clip was applied using the universal rib clip fixation plier with 3 prongs encompassing the proximal fragment and 3 prongs encompassing the distal fragment. The pliers were placed vertically to the clip, ensuring proper seating of the pliers in the centering hole, and then the clip was tightened to secure the lateral prongs around the rib.

Figure 17 Resected ribs that have been fractured and then repaired using the following methods described from top to bottom: 4 mm nylon cable tie (NCT), 2.7 mm string of pearls veterinary locking plate (SOP), 2.7 mm reconstruction plate modified to accommodate 3.2 cortical screws with cerclage wire applied (MRP), and STRACOS™ Titanium 3D rib clip (RC).

iv. Biomechanical testing of repaired ribs

Repaired ribs underwent a single-cycle to failure four-point bending test using the Instron 5565 universal materials testing machine (Instron, Norwood, Massachusetts). Force was applied to the intra-thoracic, convex surface of the rib simulating internal stresses that leads to fatigue or failure of the repair at a crosshead speed of 0.25 mm/s and center span distance of 30 mm, with a loading span of 90 mm (Figure 18c and d). F_{max} and F_{fail} of the repaired ribs were recorded. From the load-displacement curves, the stiffness (K, N/mm) was determined by calculating the slope of the linear elastic portion of the curve. Mode of failure was recorded and defined as failure at the original fracture site, screw or implant pull out, new fracture dorsal to the implant, new fracture ventral to the implant, or other fracture.

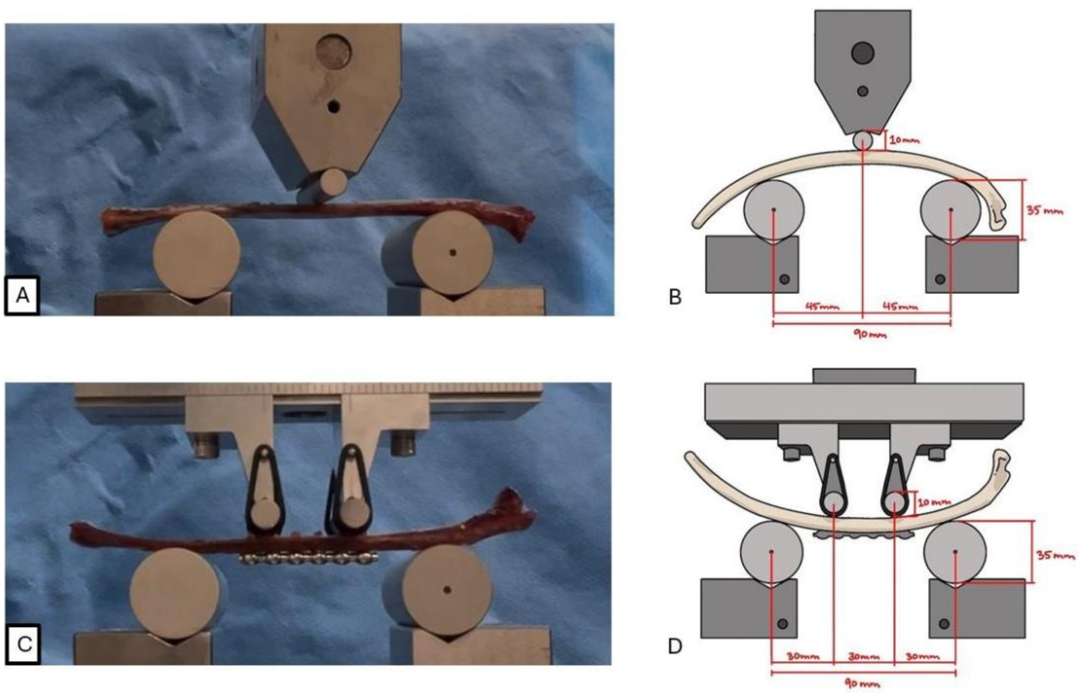

Figure 18 Biomechanical three-point testing set up to fracture intact ribs (A and B) and four-point testing set up to test repaired ribs (C and D). A string of pearls (SOP) plate for repair is shown for testing.

v. Statistical Analysis

Means and standard deviations were calculated by repair group for F_{max}, F_{fail}, and stiffness for both intact and repaired ribs. To account for repeated measurements per horse, linear mixed models were used to compare treatment means assuming a compound symmetric covariance matrix. All models adjusted treatment means for rib number (treated as a categorical variable), weight, age, and rib side (left or right). All distributional assumptions were accessed using normality probability plots and histograms. The graphs did not indicate violations of assumptions. If the linear mixed models indicated statistically significant treatment differences, post-hoc comparisons were conducted using a Bonferroni correction. All analyses used a Type I error rate of 0.05 and were programmed in SAS® 9.4. Descriptive statistics were used to report data for rib dimensions and mode of failure.

Chapter 4 Results

In total, 80 ribs underwent three-point testing to fracture the rib and 4-point testing to test each method of repair (20 ribs per group). Fifteen cadavers were needed as some ribs were not intact due to method of harvest and there was a freezer malfunction which would have resulted in a subset of thoraces undergoing an extra freeze-thaw cycle. Due to concerns for differences in tissue handling, these thoraces were excluded from further testing. To ensure appropriate representation of rib # and side of thorax (L or R) additional thoraces were needed. The cadaver study population, therefore, consisted of 14 thoroughbreds and 1 Gypsy Vanner. The median age was 2 days old (mean 2.7 ± 3.8 days) with a mean body weight of 130.8 ±21.7 lbs. The mean rib dimensions were length 185.71±25.6mm, width 15.56±14.73mm, height 6.18±0.70 mm, and circumference 36.67 ±2.50.

For intact ribs, there was no difference in F_{max} (P=0.46) or F_{fail} (P=0.35) among repair groups. For repaired ribs, there were differences in F_{max} (P<0.0001) and F_{fail} (P<0.0001) between groups (Table 1). Multiple comparison analysis with a Bonferroni correction identified differences among repair groups for both F_{max} and F_{fail}. Fracture repair with NCT produced significantly lower F_{max} and F_{fail} compared to MRP, SOP, and RC. The F_{max} and F_{fail} were significantly higher for MRP compared to RC repair, but like F_{max} and F_{fail} for SOP repair. The F_{max} and F_{fail} for RC repair were significantly higher than NCT, but significantly lower than MRP (Figure 19a and b).

For intact ribs, there was no difference in stiffness between groups (P=0.8967). For repaired groups, differences in stiffness between groups were observed (P<0.0001). Comparison analyses indicate higher stiffness in constructs repaired with the MRP and SOP than both NCT and RC. All remaining comparisons for stiffness were non-significant.

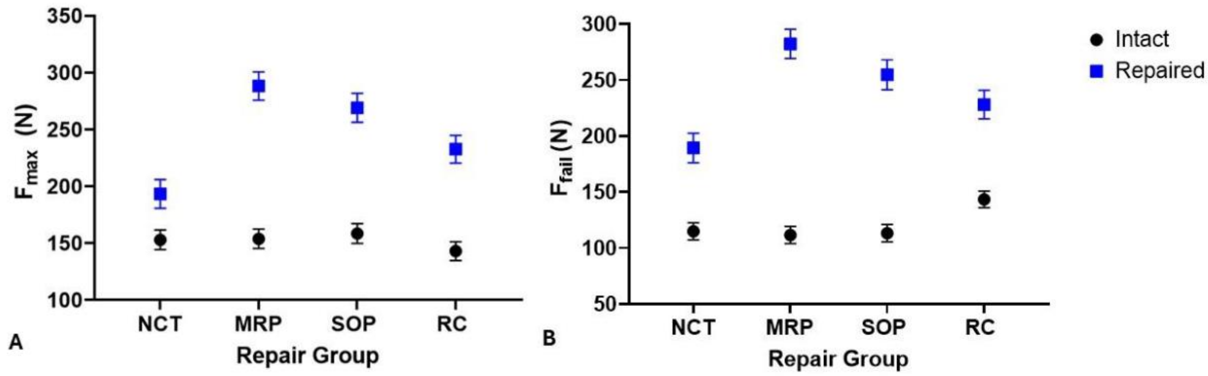

Figure 19 Fmax (A) and Ffail (B) for intact and repaired ribs for each repair group.

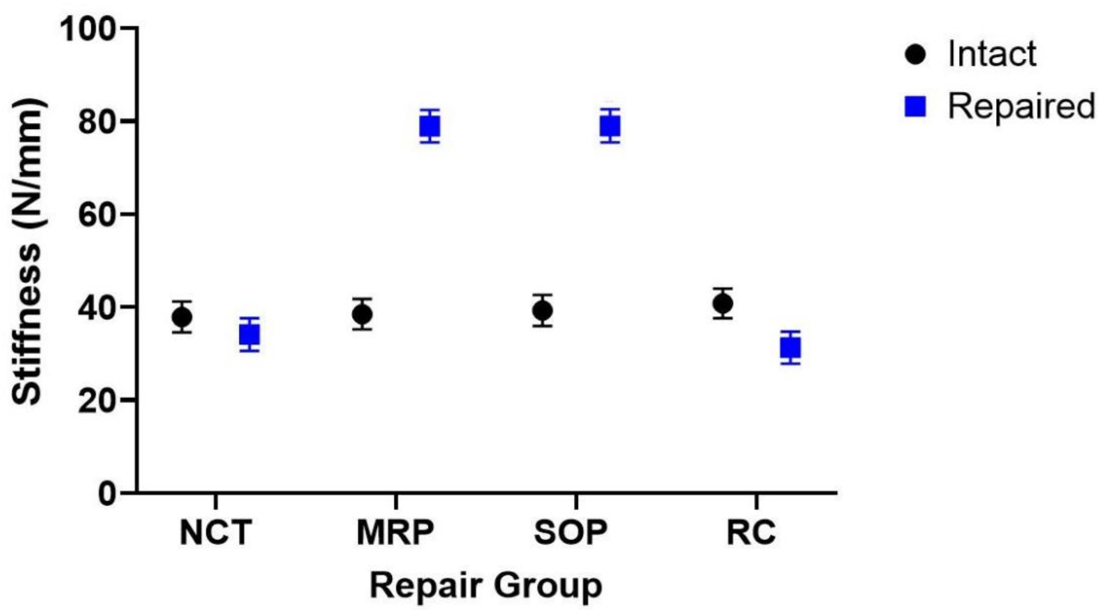

Figure 20 Stiffness (N/mm) for intact and repaired ribs for each repair group.

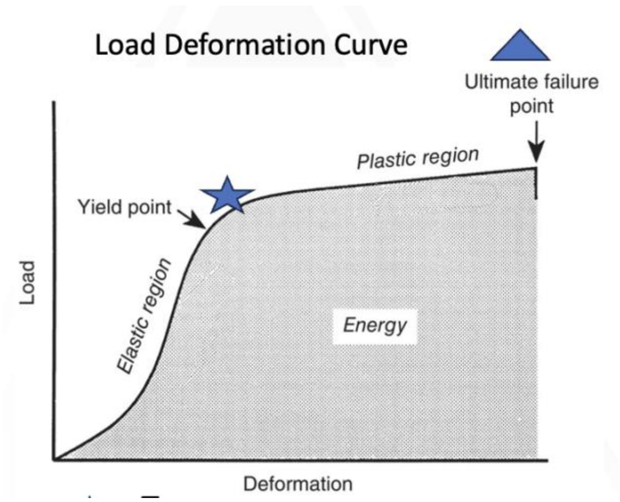

Figure 21 Load deformation curve showing the star at the F_{Max} and the triangle at the F_{Fail}.

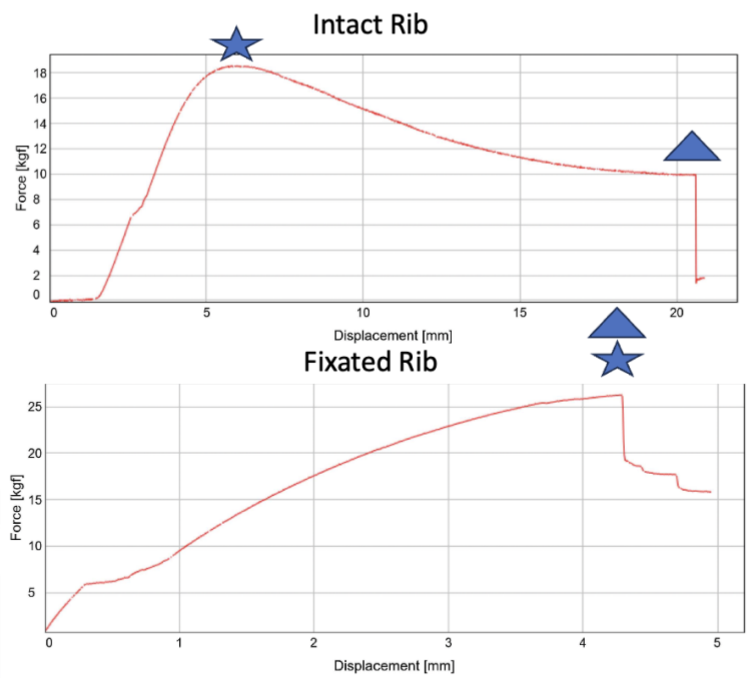

Figure 22 The top image is an intact rib and the bottom image is a fixated rib using the fixation method MRP. The star is at the F_{Max} and the triangle at the F_{Fail}.

The mode of failure was different between constructs. The NCT failed at the original fracture (11/20, 55%) or failed through a new fracture that propagated through the dorsal hole in which the NCT was coursing through (9/20, 45%). Screw pull-out occurred most in the MRP (7/20, 35%) and SOP (12/20, 60%) groups. Other modes of failure identified for MRP repair were, new fracture at the dorsal aspect of the implant (6/20, 30%), new fracture at the ventral aspect of the implant (2/20, 10%), and other new fractures (4/20, 20%). Other modes of failure for SOP were a new fracture at the dorsal aspect of the implant (3/20, 15%), a new fracture at the ventral aspect of the implant (2/20, 10%), and other new fractures (3/20, 15%). RC repair failed only at the original fracture line (20/20, 100%).

Figure 23 Fail at the original fracture line for the NCT.

Figure 24 Screw pullout in the SOP plate.

Figure 25 New fracture at the dorsal plate and bone interface in the MRP.

	Repair Group				
Outcome Variable	Nylon Cable Tie	Modified Reconstruction Plate	String of Pearls Plate	Rib Clip	P- Value
	(Mean±SEM)				
F_{max} (N)					
Intact	152.98 ± 8.62	153.87 ± 8.49	158.54 ± 8.70	143.04 ± 8.31	0.4617
Repaired	193.31 ± 12.65[2 3]	288.18 ± 12.45[1,4]	269.02 ± 12.77[1]	232.64 ± 12.19[2]	<0.0001
F_{fail} (N)					
Intact	115.01 ± 7.67	111.69 ± 7.59	113.28± 7.72	143.48 ± 7.41	0.3509
Repaired	189.55 ± 13.20[2 3]	282.36 ± 12.99[1,4]	254.83 ± 13.33[1]	228.25 ± 12.74[2]	<0.0001
Stiffness (N/mm)					
Intact	37.90 ± 3.31	38.50 ± 3.26	39.29 ± 3.35[2]	40.82 ± 3.20	0.8967
Repaired	34.12 ± 3.53[2 3]	78.93 ± 3.49[1 4]	78.98 ± 3.57 [1 4]	31.28 ± 3.44[2 3]	<0.0001

Table 1 Mean ± standard error for F_{max} (N), F_{fail} (N), and stiffness (N/mm) intact and repaired ribs. Superscripts indicate the column or repair group (1=NCT, 2= MRP, 3= SOP, 4 = RC) that is different from the referenced value within each row using Bonferroni correction.

Chapter 5 Discussion

This is the first *ex vivo* study to evaluate repair strength of four different fixation methods for equine neonatal rib fracture. Consistent with our hypothesis, rigid fixation methods (MRP and SOP) produced stronger and stiffer constructs than non-rigid fixation (NCT and RC). Failure modes also differed between fixation types with non-rigid constructs (NCT and RC) most commonly failing at the original fracture site, whereas SOP constructs primarily failed by screw pullout, and MRP exhibited variable failure modes.

All repair constructs demonstrated greater strength than intact ribs; although stiffness varied considerably between fixation methods. MRP, SOP, and RC constructs were stiffer than intact ribs, whereas NCT constructs remained comparable in stiffness to intact ribs. These findings contrast with those of a recent human rib biomechanical study, in which all constructs were less strong and less stiff than intact, non-fixated rib.[46] However, Prins et al., (2023) used ribs obtained from aged adult cadavers, while our study evaluated skeletally immature bone obtained from neonatal foals less than 2 weeks of age. Few studies have investigated the biomechanical behavior of immature ribs. Immature bone has been shown to be more porous and elastic, which means it can sustain higher loads to failure than mature bone.[47,48] In addition, there can be extreme variation in microstructure throughout the rib during growth leading to variable strength and stiffness.[49] Intact foal ribs in our study exhibited slightly higher strength and stiffness than immature porcine ribs up to six weeks of age indicating that some differences may be species related.[50] Optimal rib repair strength and stiffness are not well defined , but ideally, repair strength and stiffness should approximate that of intact bone while preserving rib cage motion to support respiratory mechanics. Repairs that are stiffer than naive bone can cause stress-shielding or stress concentration at the bone-implant interface, impairing fracture healing or causing implant failure.[51] In the study by Prins et al., plate and screw systems demonstrated the greatest stiffness, while clamping systems had lower stiffness. In our study, the NCT and RC constructs had lower stiffness than intact ribs, demonstrating the flexible, less rigid nature of these repair methods, which may be advantageous for certain rib fractures. The ideal repair should also be tailored to fracture characteristics (chronicity, configuration, number of ribs involved) and bone properties (immature versus mature or osteoporotic) to minimize hardware failure and implant-related complications.

Implant-related complications remain an important consideration in equine neonatal SSRF. Reported complications include implant migration, construct failure and screw loosening [35,45,52,53] In the present study, rigid fixation constructs most failed at the bone-implant interface, whereas non-rigid constructs failed at the fracture site itself. These differing failure patterns may influence implant selection depending on fracture characteristics.

The RC has been designed for the human adult rib, which differs in size and shape from the equine neonatal rib, therefore, the clamps did not fully contact the bone in the present study. Instead the RC encircled the rib in a cage-like configuration with minimal bone-clamp contact. This likely contributed to reduced strength and stiffness in our study. Design modifications tailored to equine neonatal ribs could improve performance, though cost considerations would need to be addressed for the veterinary market. Both the MRP and the SOP were applied using cortical screws of the same length, engaging both cortices of the rib. The comparable performance of MRP and SOP constructs was notable. Although SOP plates are designed to provide increased construct stability due to the fixed angle of fixation, superior strength was not observed in the present study. While both constructs used bi-cortical screw placement, the SOP construct used 2.7 mm cortical screws and cerclage wire was not used to augment the repair, differences that may have impacted the results when the SOP was compared to the MRP. When securing plates with screws, bi-cortical engagement is recommended for compression plating but is not necessary for locking plate constructs. A recent study in human SSRF comparing uni-cortical versus bi-cortical screw placement found no difference in construct strength or failure. In the present study, ribs were repaired with screws engaging both cortices of the bone. While descriptions in the literature are not always explicit, reported screw lengths suggest that most equine rib repairs employ bi-cortical placement. Care must be taken to avoid excessively long screws, which can damage underlying structures when placed bi-cortically. Further work to investigate uni-cortical screw placement in both reconstruction and locking plate systems to determine its effect on construct strength and failure modes in immature bone may be valuable.

Long-term outcome data for foals with rib fractures is largely limited to racing performance. Fehin et al (2017) evaluated 44 foals with rib fractures, reporting 11 foals surviving that were treated surgically and 34 foals surviving treated medically. Foals undergoing SSRF had similar return-to-racing and median earnings compared to those treated conservatively.[54] Velloso et al., (2022) assessed 73 neonates undergoing fracture repair of 1 or more ribs, comparing outcomes to their non-fractured maternal siblings. Repairs included external splints secured percutaneously with suture or cerclage wire, reconstruction plates with screws or cerclage wire, or nylon cable ties. The method of repair did not affect outcomes, with 78% of surgically treated foals surviving to discharge and 61% of these foals started a race.[45] These retrospective studies indicate that foals can survive and return to work after rib fracture repair. However, long-term data on tack-related comfort, behavior under saddle, or musculoskeletal health, including lameness, remain lacking.

This study has several limitations. Stiffness and strength of intact ribs were assessed using three-point bending because preliminary testing showed that neonate ribs were too flexible for four-point bending, with ribs bending around both top cylinders rather than fracturing along the rib. Three-point bending was chosen over standard ostectomy to evaluate the inherent biomechanical properties of naïve, intact ribs. Repaired ribs, however, were tested using four-point bending in a different orientation (extra- to intrathoracic versus intra- to extra-thoracic), preventing direct comparison with intact ribs. Fracture location differed from naturally occurring neonatal fractures to permit standardized mechanical testing. The fracture location was chosen to ensure symmetrical placement in the Instron testing machine and prevent uneven application of load. Ribs were tested under bending rather than compression to more accurately reflect lateral forces believed to cause neonatal rib fractures. Cyclic loading, which could provide more information regarding implant fatigue compared to implant failure, was not performed and should be used for testing in future studies to more accurately reflect physiologic conditions.

Furthermore, testing was performed in isolated ribs under quasi-static loading, without adjacent ribs or supporting soft tissues. In situ, fractured ribs would experience dynamic forces distributed across the rib cage, which could alter biomechanical behavior. Implants did not undergo sterilization prior to application and testing the effect of different methods of sterilization for some of the implants used has been previously evaluated and should be considered prior to use.[55] Future studies should evaluate cyclic loading, construct augmentation and screw configurations as well as in situ changes to respiratory mechanics.

Despite these limitations, this study is the first to characterize the biomechanical properties of intact equine neonatal ribs and to evaluate commonly used repair techniques, providing a foundation for further investigation and optimization of repair methods.

Chapter 6 Conclusion

In conclusion, current repair methods significantly enhance the strength of fractured equine neonatal ribs compared to naïve ribs. Repair with MRP, SOP and RC constructs also provided increased stiffness compared to intact ribs. Selection of the appropriate SSRF construct should be guided by fracture characteristics, degree of displacement, patient condition, and the clinician’s experience and available equipment.

Further research is needed to define the optimal biomechanical properties of repair constructs for equine neonates and to evaluate their impact on respiratory function, fracture healing, implant durability, and long-term patient outcomes, ultimately informing best practices for the management of neonatal equine rib fractures.

References

1. Markel MD. Bone Structure and the Response of Bone to Stress. *Equine Fracture Repair*, 2019;1-11.

2. Auer JA, Stick JA. *Equine Surgery-E-Book: Equine Surgery-E-Book*: Elsevier Health Sciences, 2018.

3. Mackie E, Ahmed Y, Tatarczuch L, et al. Endochondral ossification: how cartilage is converted into bone in the developing skeleton. *The international journal of biochemistry & cell biology* 2008;40:46-62.

4. Breeland G, Sinkler MA, Menezes RG. Embryology, bone ossification. *StatPearls [Internet]*: StatPearls Publishing, 2023.

5. Kondi S, Gowda SR. Principles of bone healing. *Surgery (Oxford)* 2023;41:625-631.

6. Radasch RM. Biomechanics of bone and fractures. *Veterinary Clinics of North America: Small Animal Practice* 1999;29:1045-1082.

7. Nordin M. Biomechanics of whole bones and bone tissue. *Basic biomechanics of the skeletal system* 1980.

8. Schwarz P. Fracture biomechanics of the appendicular skeleton: Fracture etiology and assessment. *Mechanisms of Surgical Disease in Small Animals Philadelphia, Lea & Febiger* 1991:1009-1026.

9. Markel MD. Fracture Biomechanics. *Equine Fracture Repair*, 2019;12-23.

10. Bankoff ADP. Biomechanical characteristics of the bone. *Human musculoskeletal biomechanics* 2012;61:86.

11. Markel M. Fracture biology and mechanics. *Textbook of Equine Surgery*: Saunders, Philadelphia, 1992;798.

12. Wang C, Sun CC. A critical examination of three-point bending for determining Young's modulus. *International journal of pharmaceutics* 2022;629:122409.

13. Khan Y. Characterizing the properties of tissue constructs for regenerative engineering. 2019.

14. Myers DM, McGowan SP, Taylor BC, et al. A model for evaluating the biomechanics of rib fracture fixation. *Clinical Biomechanics* 2020;80:105191.

15. Beyer B, Sholukha V, Dugailly PM, et al. In vivo thorax 3D modelling from costovertebral joint complex kinematics. *Clinical Biomechanics* 2014;29:434-438.

16. Caragounis E-C, Olsén MF, Granhed H, et al. CT-lung volume estimates in trauma patients undergoing stabilizing surgery for flail chest. *Injury* 2019;50:101-108.

17. Zhao P, Ge Q, Zheng H, et al. Clinical outcome analysis for surgical fixation versus conservative treatment on rib fractures: a systematic evaluation and meta-analysis. *World Journal of Emergency Surgery* 2025;20:10.

18. Kessel B, Dagan J, Swaid F, et al. Rib fractures: comparison of associated injuries between pediatric and adult population. *The American Journal of Surgery* 2014;208:831-834.

19. Polycarpou A, Kim BD. Pediatric surgical rib fixation: A collected case series of a rare entity. *Journal of Trauma and Acute Care Surgery* 2021;91:947-950.

20. Zhao S, Arnold M, Ma S, et al. Standardizing compression testing for measuring the stiffness of human bone. *Bone & joint research* 2018;7:524-538.

21. Keaveny TM, Pinilla TP, Crawford RP, et al. Systematic and random errors in compression testing of trabecular bone. *Journal of orthopaedic research* 1997;15:101-110.

22. Steiner M, Volkheimer D, Meyers N, et al. Comparison between different methods for biomechanical assessment of ex vivo fracture callus stiffness in small animal bone healing studies. *PloS one* 2015;10:e0119603.

23. Mischler D, Schopper C, Gasparri M, et al. Is intrathoracic rib plate fixation advantageous over extrathoracic plating? A biomechanical cadaveric study. *Journal of Trauma and Acute Care Surgery* 2022;92:574-580.

24. Joseph N, McGuinness MJ, Ratnayake M, et al. Current and Emerging Techniques for Surgical Stabilisation of Rib Fractures: A Systematic Scoping Review. *ANZ Journal of Surgery* 2026.

25. Prins JT, Van Wijck SF, Leeflang SA, et al. Biomechanical characteristics of rib fracture fixation systems. *Clinical Biomechanics* 2023;102:105870.

26. Jean D, Laverty S, Halley J, et al. Thoracic trauma in newborn foals. *Equine veterinary journal* 1999;31:149-152.

27. Velloso Alvarez A, Sandow CB, Rodgerson DH, et al. Survival and racing performance after surgical treatment of rib fractures in foals. *Veterinary Surgery* 2022;51:62-67.

28. Jean D, Picandet V, Macieira S, et al. Detection of rib trauma in newborn foals in an equine critical care unit: a comparison of ultrasonography, radiography and physical examination. *Equine veterinary journal* 2007;39:158-163.

29. Bellezzo F, Hunt R, Provost P, et al. Surgical repair of rib fractures in 14 neonatal foals: case selection, surgical technique and results. *Equine veterinary journal* 2004;36:557-562.

30. Watkins J. Etiology, diagnosis, and treatment of long bone fractures in foals. *Clinical Techniques in Equine Practice* 2006;5:296-308.

31. Griffith J, Rainer T, Ching A, et al. Sonography compared with radiography in revealing acute rib fracture. *AJR American journal of roentgenology* 1999;173:1603-1609.

32. Partlow J, David F, Hunt LM, et al. Comparison of thoracic ultrasonography and radiography for the detection of induced small volume pneumothorax in the horse. *Veterinary Radiology & Ultrasound* 2017;58:354-360.

33. Sprayberry KA. Ultrasonographic Examination of the Equine Neonate: Thorax and Abdomen. *Vet Clin North Am Equine Pract* 2015;31:515-543.

34. Çelik A, Akoglu H, Omercikoglu S, et al. The Diagnostic Accuracy of Ultrasonography for the Diagnosis of Rib Fractures in Patients Presenting to Emergency Department With Blunt Chest Trauma. *J Emerg Med* 2021;60:90-97.

35. Garrett KS, Embertson RM, Hopper SA, et al. Preoperative computed tomographic evaluation of neonatal foals with rib fractures. *Veterinary Surgery* 2022;51:816-826.

36. McCoy AM, Bishop R. Congenital and acquired musculoskeletal disorders in the neonatal foal. *Equine neonatal medicine* 2024:976-991.

37. Rogers C, Gee E, Bolwell C. EARLY EXERCISE IN THE JUVENILE HORSE TO OPTIMISE PERFORMANCE LATER IN LIFE. *BREEDING, HEALTH DISORDERS AND EFFECTS ON PERFORMANCE AND BEHAVIOR*:1.

38. Majeed FA, Zafar U, Imtiaz T, et al. Rib fixation versus conservative management of rib fractures in trauma patients. *Journal of Ayub Medical College Abbottabad* 2018;30:575-583.

39. van Loon J, Verhaar N, van Den Berg E, et al. Objective assessment of acute pain in foals using a facial expression-based pain scale. *Animals* 2020;10:1610.

40. Levine D. Fractures of the Ribs. *Fractures in the Horse* 2022:739-746.

41. Kraus BM, Richardson DW, Sheridan G, et al. Multiple rib fracture in a neonatal foal using a nylon strand suture repair technique. *Veterinary Surgery* 2005;34:399-404.

42. Downs C, Rodgerson D. The use of nylon cable ties to repair rib fractures in neonatal foals. *The Canadian Veterinary Journal* 2011;52:307.

43. Ahern BJ, Levine DG. Multiple rib fracture repair in a neonatal Holstein calf. *Veterinary Surgery* 2009;38:787-790.

44. Williams TB, Williams JM, Rodgerson DH. Internal fixation of fractured ribs in neonatal foals with nylon cable tie using a modified technique. *The Canadian Veterinary Journal* 2017;58:579.

45. Velloso Álvarez A, Sandow CB, Rodgerson DH, et al. Survival and racing performance after surgical treatment of rib fractures in foals. *Veterinary Surgery* 2022;51:62-67.

46. Prins JTH, Van Wijck SFM, Leeflang SA, et al. Biomechanical characteristics of rib fracture fixation systems. *Clinical Biomechanics* 2023;102:105870.

47. Agnew AM, Moorhouse K, Kang Y-S, et al. The Response of Pediatric Ribs to Quasi-static Loading: Mechanical Properties and Microstructure. *Annals of Biomedical Engineering* 2013;41:2501-2514.

48. Agnew AM, Schafman M, Moorhouse K, et al. The effect of age on the structural properties of human ribs. *Journal of the Mechanical Behavior of Biomedical Materials* 2015;41:302-314.

49. Agnew AM, Moorhouse K, Kang Y-S, et al. The response of pediatric ribs to quasi-static loading: mechanical properties and microstructure. *Annals of biomedical engineering* 2013;41:2501-2514.

50. Beadle N, Burnett TL, Hoyland JA, et al. A novel ex vivo model of compressive immature rib fractures at pathophysiological rates of loading. *Journal of the Mechanical Behavior of Biomedical Materials* 2015;51:154-162.

51. Chmielewska A, Dean D. The role of stiffness-matching in avoiding stress shielding-induced bone loss and stress concentration-induced skeletal reconstruction device failure. *Acta Biomaterialia* 2024;173:51-65.

52. Downs C, Rodgerson D. The use of nylon cable ties to repair rib fractures in neonatal foals. *Can Vet J* 2011;52:307-309.

53. Downs C, Rodgerson DH. How to repair fractured ribs in neonatal foals using nylon cable ties. 2008.

54. THORACIC UGTRA. The future racing performance of neonatal thoroughbreds diagnosed with rib fractures treated both surgically and conservatively. *Equine Veterinary Journal* 2017;49:5-29.

55. Sicard GK, Hayashi K, Manley PA. Evaluation of 5 types of fishing material, 2 sterilization methods, and a crimp-clamp system for extra-articular stabilization of the canine stifle joint. *Vet Surg* 2002;31:78-84.

56. Worn M, Jones MD. Rib fractures in infancy: establishing the mechanisms of cause from the injuries—a literature review. Medicine, science and the law. 2007;47(3):200-12.
57. Bauman ZM, Tian Y, Doben AR, Schubl SD, Pieracci FM, Kaye AJ, et al. Chest Wall Injury Society guidelines for surgical stabilization of rib fractures: Indications, contraindications, and timing. Journal of Trauma and Acute Care Surgery. 2025;99(4).
58. Prins JTH, Wijffels MME, Pieracci FM. What is the optimal timing to perform surgical stabilization of rib fractures? J Thorac Dis. 2021;13 (Suppl 1):S13-s25.
59. Marieb, E. N., & Hoehn, K. (2019). Human Anatomy & Physiology (11th ed.). Pearson.